Journal of Atmospheric Chemistry **32:** 327–356, 1999.

The Role of Multiphase Chemistry in the Oxidation of Dimethylsulphide (DMS). A Latitude Dependent Analysis

F. CAMPOLONGO[1], A. SALTELLI[1], N. R. JENSEN[2], J. WILSON[3] and J. HJORTH[2]

[1]*Institute for Systems, Informatics and Safety, Joint Research Centre, TP 361, 21020 Ispra (VA), Italy*
[2]*Environment Institute, Joint Research Centre, TP 272, 21020 Ispra (VA), Italy*
[3]*Environment Institute, Joint Research Centre, TP 460, 21020 Ispra (VA), Italy*

(Received: 10 June 1998; in final form: 12 October 1998)

Abstract. A kinetic model for the OH-initiated homogeneous gas phase oxidation of dimethylsulfide (DMS) in the atmosphere (Saltelli and Hjorth, 1995), has been extended here to include the liquid phase chemistry. The updated model has then been employed to predict the temperature dependency of the MSA/nss-SO_4^{2-} ratio. Model predictions have been compared with observational data reported in Bates *et al.* (1992). Sensitivity and uncertainty analysis has been performed in a Monte Carlo fashion to identify which are the important uncertainties on the input parameters and which are the possible combinations of parameter values that could explain the field observations. Results of the analysis have indicated that the temperature dependencies of the interactions between gas phase and liquid phase chemistry may to a large extent explain the observed T-dependence of the MSA/nss-SO_4^{2-} ratio. The potential role of multi-phase atmospheric chemistry, not only in the case of SO_2 but also of other oxidation products of DMS and, particularly, of DMS itself, has been highlighted.

Key words: DMS oxidation, sulphur dioxide, methane sulphonic acid, non-sea-salt sulphate, multi-phase atmospheric chemistry, temperature dependency analysis, uncertainty analysis, sensitivity analysis.

1. Introduction

Recently, it has been proposed that the forcing due to aerosols is comparable in magnitude to current anthropogenic greenhouse gas forcing but opposite in sign (Charlson *et al.*, 1992; Penner *et al.*, 1991, 1992). However, uncertainties in the forcing due to aerosols and the effect on cloud albedo are much larger than in the case of the greenhouse gases, and the distribution of the aerosols shows much larger geographical variability than that of the greenhouse gases.

Emissions of dimethyl sulphide (DMS) clearly gives an important contribution to aerosol formation and thus to radiative forcing (direct as well as indirect through the formation of cloud condensation nuclei) in remote marine areas (Shaw, 1983;

Charlson *et al.*, 1987; Bates *et al.*, 1987; Schwartz, 1988). DMS may also be a source of particles in the free troposphere which, in turn, can influence particle concentrations in the boundary layer by entrainment (Raes, 1995). Large amounts of DMS are emitted into the atmosphere each year by phytoplankton in the oceans. DMS is the major natural source of sulphur to the atmosphere with an emission of 12–54 Tg yr^{-1} (Andreae, 1990; Spiro *et al.*, 1992; Bates *et al.*, 1992), and it accounts for 10 to 40% of the total gaseous sulphur emitted into the atmosphere. In the atmosphere DMS is oxidised mainly by the OH and NO_3 radicals to form the several sulphur containing products, such as sulphur dioxide, methane sulphonic acid, and sulphuric acid (Yin *et al.*, 1990a,b; Tyndall and Ravishankara, 1991; Jensen *et al.*, 1992). It has been hypothesised that emissions of DMS would interact with climatic changes (Charlson *et al.*, 1987), possibly attenuating warming by greenhouse gas forcing. However, this hypothesis has been recently questioned on the basis of El Niño observations (Bates and Quinn, 1997).

To accurately evaluate the magnitude of the contribution of DMS to aerosol formation, a good understanding of the atmospheric chemistry of DMS is needed. However, in spite of many research efforts including laboratory, field and modelling work, the atmospheric processes involved in the oxidation of DMS are still only understood at the level of various hypotheses for mechanisms that possibly could explain the observations that have been made in the field.

The contribution to the modelling efforts of Yin *et al.* (1990a,b) have been particularly important. Later contributions are to a large extent based on chemical reaction schemes that are modified versions of the large reaction scheme presented by Yin *et al.* (Koga and Tanaka, 1993, 1996; Hertel *et al.*, 1994; Ayers *et al.*, 1996). A detailed discussion of the possible temperature dependencies of the DMS oxidation mechanism has been presented by Barone *et al.* (1995).

As discussed by Ayers *et al.* (1996) the ratio between methane sulphonate (MSA) and non-seas-salt sulphate (nss-SO_4^{2-}) seems to offer the best opportunity for comparing observed data to those predicted by models, in particular for what concerns the temperature dependencies involved in the oxidation processes. Further, this ratio may be used for estimating the actual contribution of DMS to the observed nss-SO_4^{2-} from measurements of MSA, if the dependence of the ratio on temperature and other ambient conditions are sufficiently well known (Saltzman *et al.*, 1986; Savoie and Prospero, 1989).

An evaluation and sensitivity analysis of available mechanisms for the atmospheric chemistry of DMS has been published recently by Capaldo and Pandis (1997), in which the oxidation schemes of Yin *et al.* (1990a,b), Koga and Tanaka (1993), Hertel *et al.* (1994), Benkovitz *et al.* (1994) and Pham *et al.* (1995) are discussed and compared to field observations. The study indicates that the variations among parameterised and comprehensive gas phase mechanisms are small and more relevant to SO_2 and MSA than to nss-sulphate predictions, which is more sensitive to the uncertain parameterisation of heterogeneous processes.

The present study further explores the potential role of multiphase chemistry, focussing on the temperature dependency of the MSA/nss-SO_4^{2-} ratio. It is sought to identify which parameters could possibly explain the observed values through a sensitivity and uncertainty analysis. We have considered not only the temperature dependencies involved in the gas phase chemistry but also expected temperature dependencies of the interactions between gas phase and liquid phase chemistry. The analysis indicates that these latter temperature dependencies may to a large extent explain the actually observed ones of the MSA/nss-SO_4^{2-} ratio. Thus the present analysis highlights the potential role of multiphase atmospheric chemistry not only in the case of SO_2 but also of other oxidation products of DMS and, particularly, of DMS itself. The model does not consider the possible, but very uncertain, contributions of other species than OH, such as NO_3 radicals, BrO or Cl atoms, to the oxidation of DMS in the atmosphere. Neither does it consider liquid phase reactions of other sulphur-containing intermediates in the oxidation process than DMSO, $DMSO_2$ and MSA, although laboratory studies suggests that such reactions occur and may be relevant, e.g., in the case of $CH_3S(O)_xOONO_2$ (Van Dingenen *et al.*, 1994). Also reactions of water soluble intermediates such as hydroperoxides or methane sulphinic acid (Sørensen *et al.*, 1996) are potentially important, but the present understanding of this chemistry is very limited.

Finally, the potentially important sink for SO_2 represented by uptake and reaction on sea salt aerosol and subsequent deposition of this (Chameides and Stelson, 1992) has not been included in the model due to the difficulties in making a quantitative evaluation of its importance on a latitudinal basis. In addition to acting as a sink for SO_2 this would also cause a somewhat enhanced conversion rate of SO_2 to sulphate. According to the estimate by Chameides and Stelson, this sink for SO_2 would be of approximately the same magnitude as dry deposition. A sink for SO_2 will lead to an increase in the ratio $[MSA]/([SO_2] + [H_2SO_4])$ which is evaluated in the present study, but to understand the overall impact on this ratio also the potential removal of MSA by uptake on sea-salt surfaces must be taken into account.

2. Model Description

To study the temperature dependency of the MSA/nss-SO_4^{2-}, the dimethyl sulphide KInetic Model (KIM) is employed in this work. The KIM model was developed by Saltelli and Hjorth to analyse the chemical mechanisms involved in the atmospheric oxidation of DMS. The model treats only the gas phase chemistry of DMS and its sulphur-containing oxidation products; the concentrations of other relevant trace gas species are not variables calculated by the models but externally controlled variables. Two aspects should be highlighted:

- the reaction scheme adopted in the model was affected by large uncertainty (structural uncertainty), and

– the error bars associated with the rate constants governing DMS oxidation kinetics were uncertain as well, and in some instances almost arbitrary (parametric uncertainty).

These concerns, together with the scarcity of observed data for a proper model calibration, led to the implementation of a model building process where uncertainty and sensitivity analysis played a central role.

Uncertainty Analysis (UA) refers to an assessment of the uncertainty in analysis outcomes that derives from uncertainty in analysis inputs. By assigning a range of uncertainties to the input parameters, and performing a Monte Carlo (MC) analysis,* the mean value of the model prediction and, more in general, the output distribution function, can be estimated (Helton, 1993).

Sensitivity Analysis (SA) refers to an assessment of the contributions of individual analysis inputs to the total uncertainty in the output of the analysis. One possible goal of SA could be to quantify the percentage of the total output variance that each parameter, or combination of parameters, is accounting for.

In other words: Sensitivity Analysis encourages investigating the relevance of the various processes modelled and is used to determine which processes should be further studied; UA has a complementary role contributing the final stage estimates of uncertainties on predictions. For a review and comparison of UA/SA techniques see Iman and Helton (1988), Helton *et al.* (1991), Helton (1993), Saltelli and Marivoet (1990), Saltelli and Homma (1992), Saltelli *et al.* (1993), Turanyi, (1990).

The performance of SA in the model building exercise is usually an iterative process: once the SA has been performed, and the most influential input variables and parameters have been identified, their values can be consequently calibrated to reach a good agreement between model predictions and observed values.

The MC analysis by Saltelli and Hjorth (1995) has allowed:

1. the uncertainty in model prediction (in particular the gas phase ratio MSA/$(SO_2 + H_2SO_4)$ concentration at a given time) to be estimated;
2. the relative importance of each input parameter in determining (1) above to be quantified.

One of the main limitations of the studies done with KIM was the neglect of temperature effects on the DMS-oxidation process. In 1994, Remedio *et al.* extended the model to include the latitude dependency, considering not only the latitudinal differences in terms of temperature and trace gas concentrations (e.g., O_3, OH, DMS, NO_x), but also taking into account the diurnal cycles of these parameters. The Monte Carlo analysis was then performed again latitude by latitude, by reading average temperatures and trace gases' concentration from the output of a general circulation model, Moguntia (Zimmermann, 1984; Zimmermann *et al.*, 1989). This

* Monte Carlo is but one of the possible methods to implement an uncertainty analysis. For a review, see Helton 1993.

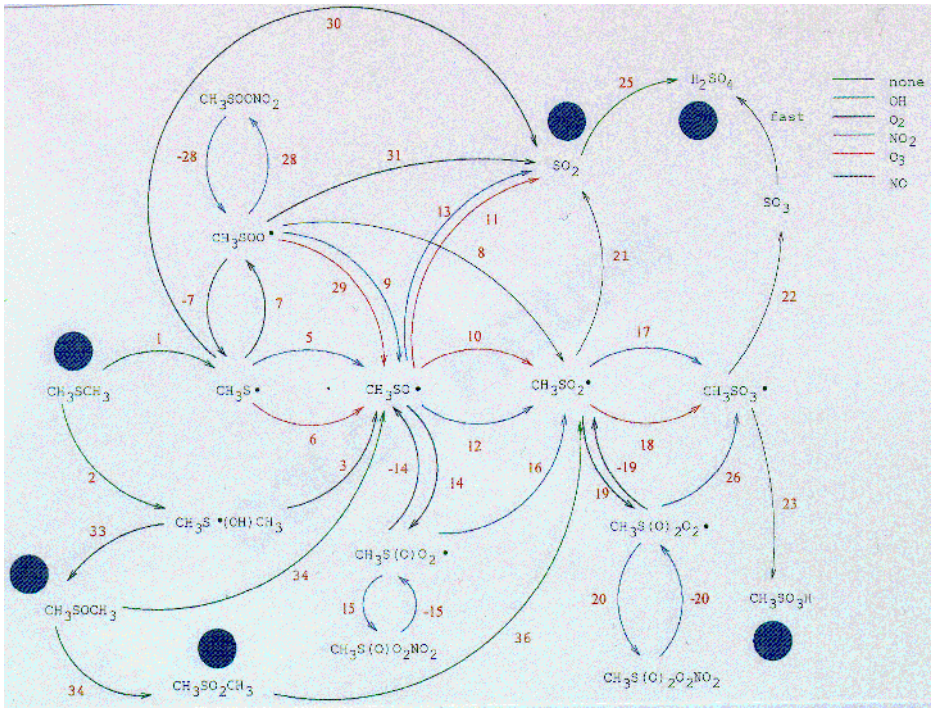

Figure 1. The homogeneous chemistry scheme adopted with minor modifications from Saltelli and Hjorth (1995). The reactions involved in this scheme are listed in Table I.

has allowed the analysis of the possible regional differences on the main oxidation pathways of DMS and of the relative amounts of end-products formed.

Another important development was the inclusion of the multiphase (air/droplet) chemistry and dry deposition, apparently the largest sink for SO_2 molecules. In the present article the multiphase chemistry is dealt with, and a first, crude representation of cloud processing.

Uncertainties in the understanding of the mechanisms of the oxidation of DMS and of its intermediates in liquid phase are even more severe than for the homogeneous chemistry mechanism. This justifies the UA, SA based approach to model building to be extended to the scope of the present work.

3. Methods

The present version of the KIM model results from the integration of system analysis computational features with modelling of chemical kinetics and mass transfer. The homogeneous chemistry scheme, adapted with minor modifications from Saltelli and Hjorth (1995), is given in Figure 1. The hypothesised heterogeneous chemistry reactions are outlined in Figure 2. In Table I, in Appendix A, can be found the chemical kinetic data applied in the mechanism that was used

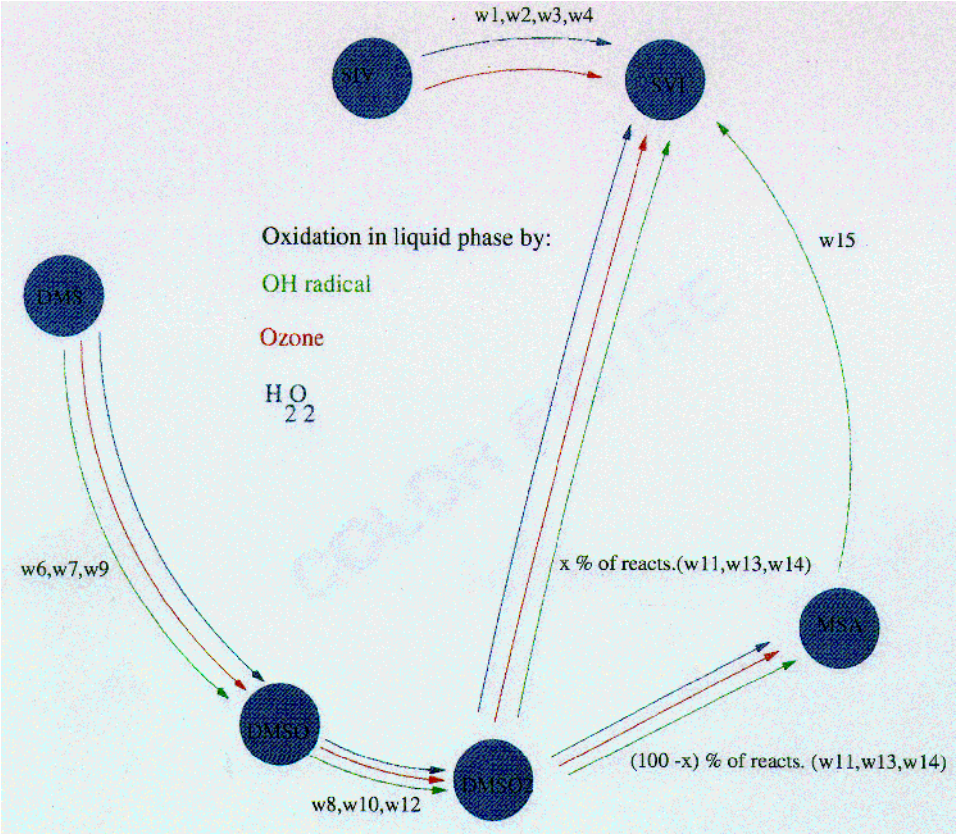

Figure 2. The heterogeneous chemistry scheme. In the liquid phase oxidation takes place through chemical reactions based on O_3, H_2O_2, and OH radicals. While the oxidation of SIV (which includes SO_2, HSO_3^-, and SO_3^{2-}) to SVI (H_2SO_4) is relatively well known (Seinfeld, 1986), the liquid phase chemistry of DMS, DMSO, and $DMSO_2$ is subject to speculation. The reactions involved in this scheme are listed in Table I. SIV $=$ {SO_2, HSO_3^-, SO_3^{2-}}; SVI $=$ {H_2SO_4}.

for the investigation. Table I includes gas phase reactions, liquid phase reactions, gas/liquid phase equilibrium constants (Henry's Law constants) as well as the temperature dependencies of these parameters. Sources of information for all the data in Table I are also reported (see list of references in Appendix A).

Other features of the new version of the KIM model are described below.

3.1. STATISTICAL SUBROUTINES

The KIM model is embedded in a Monte Carlo driver. This is composed of a pre- and a post-processor (PREP and SPOP, respectively). The PREP pre-processor is a FORTRAN utility to assist in the implementation of a Monte Carlo analysis (Homma and Saltelli, 1991). This analysis implies that a given model, coded into a computer program, is run for several combinations of input parameter values, in order to gain insight both on the distribution of value of the model output (prediction) and on the relationship between output uncertainty and uncertainty on the individual parameter. The SPOP (Statistical POst Processor) code performs uncertainty and sensitivity analyses (Saltelli and Homma, 1991) on a sample output from a Monte Carlo simulation. The sample contains values of the output variable (in the form of a time series) and values of the input variables for a set of different simulations (runs), which are realised by varying the model input parameters.

3.2. MODELLING t-DEPENDENT UNCERTAIN PARAMETERS

In KIM some of the parameters are at the same time uncertain and temperature dependent; typically, the T-dependence of a rate constant involves poorly known activation energy and/or pre-exponential factors.

As a result, a problem arises given that the Monte Carlo sampling matrix is generated only once, at the beginning of the simulation. This matrix drives the selection of a particular value for a given parameter (say R) for a given run and keeps it fixed all the way through the simulation. If, in the course of the individual run, the temperature changes, we need to change the value of R consequently. To do this without re-sampling a new value, the cumulative distribution functions (CDF's) are drawn for any uncertain T-dependent parameters (see Figure 3). Hence, in generating the Monte Carlo sampling matrix, we did not sample directly a value for the parameter R, but a value for the quantile Q of its distribution. Then, given the Q value sampled, the value of the parameter (R in the figure) can then be derived at any temperature from the CDF. This allows to changing the R-value during an individual run, while T changes, still keeping fixed the Q value sampled in the Monte Carlo matrix.

In the present investigation, temperature diurnal variations were not taken into account and the temperature was kept constant within the 24 hours of each simulation.

3.3. MODELLING THE KINETIC CONSTANT k_{21}

Results of the previous sensitivity studies on KIM (Remedio *et al.*, 1994) confirmed the latitude dependence of the hypothesised reaction pathways and its temperature dependence. The kinetic constant k_{21} (the rate coefficient of the reaction $CH_3S(O)_2 \rightarrow CH_3 + SO_2$), which dramatically depends on temperature, was one of the most influential factors on the system.

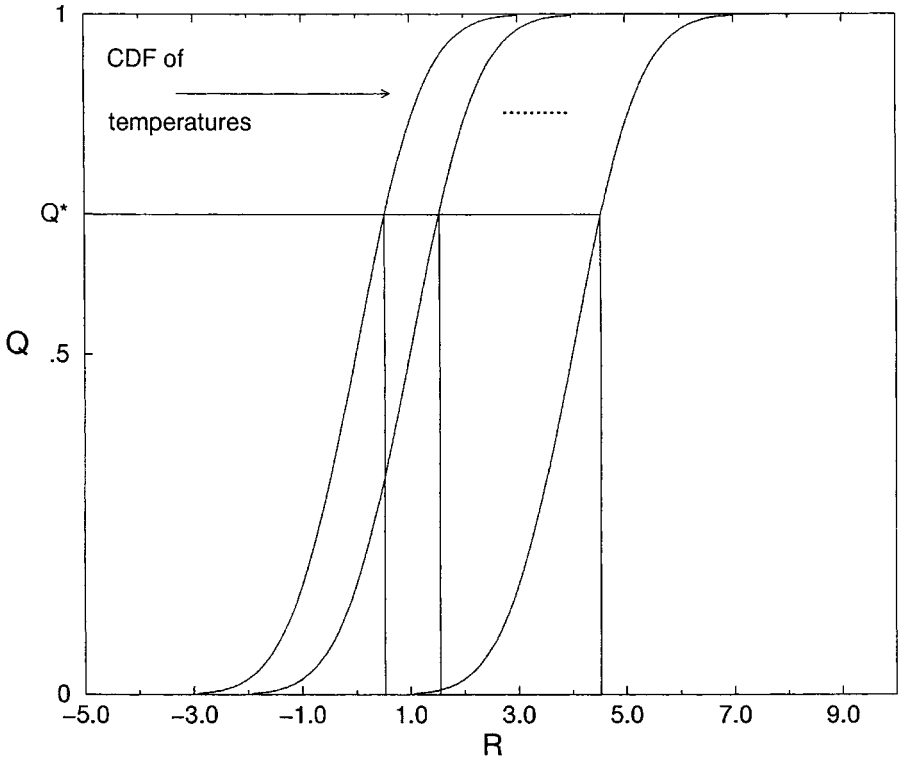

Figure 3. The cumulative distribution functions (CDF's) for the uncertain T-dependent parameters. Given a sample value for the quantile Q, the value of the parameter R can be determined at any temperature.

In this study, on the base of new available data, the original (Saltelli and Hjorth, 1995) uniform distribution function assumed for k_{21}, was replaced by a normal distribution (adopted from Ray *et al.*, 1996) with average $k_{21}(T)$ and standard deviation std($k_{21}(T)$), respectively, of the form

$$k_{21}(T) = A \exp\{-E/(RT)\},$$

$$\text{std}(k_{21}(T)) = f_{298K} * \exp\left(\Delta E/R * \left(\frac{1}{T} - \frac{1}{298K}\right)\right),$$

where $E = 18000$ cal mol^{-1}, $\Delta E = 1510$ cal mol^{-1}, $A = 8.1 \times 10^{15}$ s^{-1}, and $f_{298K} = 1.59$ (see also Appendix A, Table I, comment C21).

3.4. MODELLING THE MULTIPHASE CHEMISTRY

The impetus to the introduction of multiphase chemistry was to assess the rate of the oxidation of SO_2 to H_2SO_4, where both gas phase and liquid phase processes

are at work, as well as the potential role of liquid phase chemistry in the oxidation of organic sulphur species.

In the present version of the model, a mono-disperse population of droplets has been assumed, all of the same (average) radius of 0.015 mm, the number of droplets depending on the relative humidity (input). Henry's law governs the flux of each diffusing species into the droplet. Referring to Figure 1 the sphere highlight the entry point for gas to liquid migration (i.e., which species diffuse to the droplets). The drops are assumed as perfectly mixed, and the Henry's law is used to impose, given a species concentration in the liquid phase, the gas phase concentration of the same species at the drop surface. Gas phase diffusion governs then the flow of the species. The relative equations are

$$X_A^a = \frac{1}{H_A P}[A_{\text{aq}}] \tag{3.1}$$

$$\frac{d[A]}{dt} = \frac{3cD}{a^2} \ln\left(\frac{1 - X_A^0}{1 - X_A^a}\right), \tag{3.2}$$

where A is the name of the species, $\lfloor A_{\text{aq}} \rfloor$ is the aqueous concentration of species A, a is the radius of the droplet in cm, X_A^a is the mole fraction of species A at the drop surface, X_A^0 the same mole fraction far away from the drop, P is the atmospheric pressure in Atm, D is the diffusivity of the species in gasphase in cm^2/s, c is the total number of molecules per cubic centimetre in the gas phase, and H is the Henry's law constant in M atm^{-1} (Byrd *et al.*, 1970).

The differential equations for the species concentration in the droplet is computed following the scheme outlined by Seinfeld (1986) for the simpler case not including DMS and its intermediates. The system is solved by combining Equations (3.1) and (3.2) with the kinetic equations (Table I in Appendix A), the mass balance, and the electro-neutrality condition.

The model comprehends liquid phase oxidation by reaction with O_3, H_2O_2 and the OH radicals. The OH radical concentration was not controlled by gas-liquid phase exchange. Different concentrations in the range 2.5×10^{-15}–2.5×10^{-13} M were applied but no relevant changes in the output concentrations of sulphur compounds were observed. While the oxidation of SIV to SVI is relatively well understood (Seinfeld, 1986), the liquid phase chemistry of DMS, DMSO and $DMSO_2$ is object of speculation. In our scheme (Figure 2) we have assumed that DMS is oxidised to DMSO, which is further oxidised to $DMSO_2$. For the latter compound, both the pathways assumed to lead to formation of sulphuric acid and to formation of MSA are included. The relative importance of fluxes, governed by the kinetic constants k_{11}, k_{13} and k_{14} in the scheme, are split onto two different paths:

- 66% of the total flux is going from $DMSO_2$ to SVI
- the remaining 34% is going from $DMSO_2$ to MSA.

Percentages were estimated on the basis of data reported in Bates *et al.* (1992), i.e., trying to get the best agreement between the value of the ratio MSA/nss-SO_4^{2-} predicted by the model, and the value experimentally observed by Bates *et al.* (1992), at the temperature $T = 298\,^{\circ}\mathrm{K}$.

There may well be other pathways from DMSO to MSA than the one assumed in the present model; in fact, as discussed in the recent work of Jefferson *et al.* (1998) and of Davis *et al.* (1998), there is evidence, that the OH-initiated oxidation of DMSO forms methane sulphinic acid which then can be further oxidised to MSA. If this is the main reaction pathway, $DMSO_2$ concentrations would be overestimated by the present model but the description of the kinetics of MSA-formation would remain essentially unchanged.

Note that the heterogeneous chemistry scheme derived here is depending on the choice of the k_{21} value. In fact, a change in the value of k_{21}, would result in a change of the values predicted by the model (for the ratio MSA/nss-SO_4^{2-}) at $T = 298\,^{\circ}\mathrm{K}$, and consequently in the values estimated for the percentages in the scheme.

3.5. MODELLING THE CLOUD DYNAMICS

Among the limitations of the previous versions of the KIM model, the non-inclusion of the dynamic behaviour of clouds – especially cloud processes such as condensation and evaporation cycles – was thought to have a large influence on the behaviour of the system. Nevertheless a coupling of the full chemistry of KIM with our cloud dynamics module (Remedio *et al.*, 1994) would increase the complexity of the system to a level unsuitable – at present – for our system analysis approach. Thus, an attempt was made to include some dynamics into KIM reproducing the variability of the clouds within the typical 24 hours covered by the computation. This was done via a Monte Carlo approach: The cloud behaviour within a day was simulated acting on the water liquid content (variable WATLIQ). WATLIQ value was kept constant within a run, but varied from run to run in a Monte Carlo fashion. For WATLIQ, a log-uniform distribution between 1×10^{-7} and 5×10^{-5} (Pruppacher and Klett, 1980) was chosen. The average of the results over several runs was taken as representative of the variable behaviour of clouds.

3.6. MODELLING DRY AND WET DEPOSITION FOR THE SO_2

The effect of rain has also been added to the system. Rain is assumed to fall once every ten days (a variable called RAIN and following a uniform distribution in the set of integers $(1, \ldots, 10)$ is added) and its effect on the system is simulated by wet removal of all sulphur species.

Furthermore, dry deposition of the SO_2 was also modelled. The value of the SO_2 deposition velocity was taken from Luria *et al.* (1991).

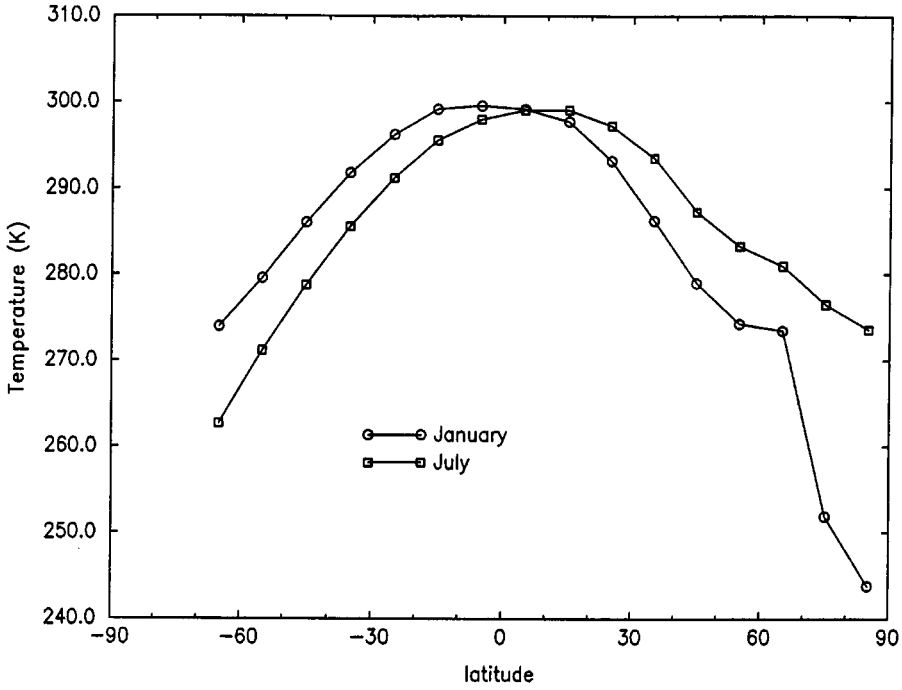

Figure 4. MOGUNTIA mean monthly air temperature (100–950 mbar) zonally averaged over all oceanic (no land) grid elements. Data from Oort *et al.*, (1983).

3.7. COUPLING WITH MOGUNTIA

For the latitude dependency study the model was coupled 'offline' with a general circulation model (MOGUNTIA, Zimmerman *et al.*, 1984, 1989) in order to generate the latitude dependent variables (temperature, trace gases concentration).

Temperature. Zonally averaged monthly mean surface temperatures over the sea, were extracted from the climatological datasets used by the MOGUNTIA model. MOGUNTIA is a 3-D Eulerian global tracer transport model, with a resolution of 10×10 degree $\times$ 100 hPa resolution. In the model, both the transport and the principal synoptic variables are represented by monthly mean values which have been derived from synoptic observations over a 15 year (1958–1973) period (Oort, 1983). The zonal average temperature profiles for January and July are illustrated in Figure 4.

Trace gases. A version of the MOGUNTIA model, in which models of the atmospheric nitrogen (Dentener, 1993) and sulphur (Langner and Rodhe, 1991) cycles have been combined (Dentener, 1994) was used to generate zonal average surface concentration fields over the oceans, for the NO_x species, the oxidants OH and O_3, and DMS. These are illustrated in Figure 5. Since in our experiments we simulated the winter season, data illustrated in the figure are the ones of the month of January. In addition, the zonal average DMS emissions from the oceans used in

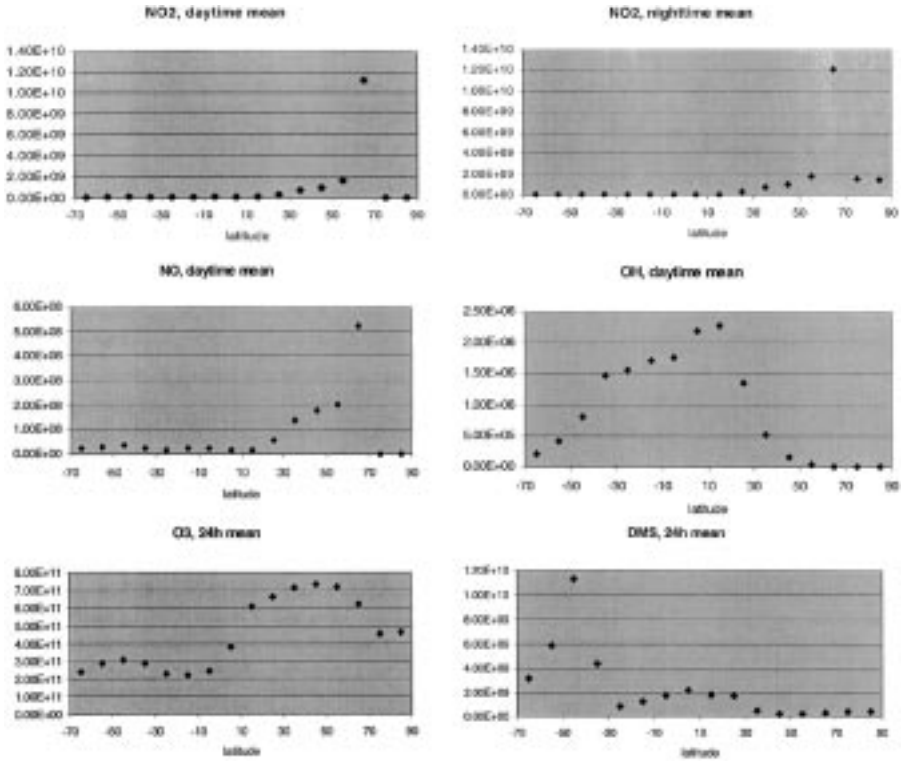

Figure 5. January mean zonal average oceanic concentration fields (molecules cm^{-3}) as calculated by full chemistry version of MOGUNTIA (Dentener, private comunication, 1994). Data are for the 16, zonal 10 degree intervals containing oceans.

the sulphur chemistry model (Langner and Rodhe, 1991) have been used in the flux calculation studies.

4. Results and Discussion

Published results on the ratio in marine aerosol between MSA and non-sea-salt sulphate (MSA/nss-SO_4^{2-}), are available from several field measurements. DMS oxidation is believed to be the predominant source of non-sea-salt-sulphate (nss-SO_4^{2-}) at remote marine sites and the only relevant source of MSA. Hence, the values of the ratio [MSA]/[nss-sulphate] observed at remote marine sites should reflect, essentially, DMS chemistry only. We have thus used a comparison between observational data and model output to corroborate the reaction mechanisms applied, with a focus on the dependence on latitude, i.e., principally, on temperature (Bates *et al.*, 1992). For this exercise, we have chosen to apply the simple linear relationship between temperature and [MSA]/[nss-sulphate] which Bates *et al.* (1992) found to be a good approximation to the observed values in unpolluted (Southern Hemisphere) marine sites. The observed values reported in Bates *et*

al. (1992), are taken from various author's work and are characterised by a large variability because they represent different 'snapshots' of atmospheric conditions (especially with respect to cloud cover and insolation). Nevertheless, the linear relationship found by Bates has a value of $R^2 = 0.87$ which confirms the validity of the regression. Furthermore, measurements of the MSA/nss-SO_4^{2-} ratio at three coastal Antarctic stations reported in a very recent paper by Legrand and Pasteur (1998) are in good agreement with the values derived by using the relationship proposed by Bates *et al.* (1992).

Sensitivity and uncertainty analyses have allowed the identification of the parameter values that should possibly be revised if the agreement between model and reality were to be improved. For the Monte Carlo statistical analysis, each model run covered 24 hours in order to reduce computing time to an acceptable level. Since within 24 hours we do not achieve a steady state concentration of sulphate but tend to underestimate its concentration and overestimate that of SO_2, we have chosen to compare observed values of [MSA]/[nss-sulphate] to modelled values of [MSA]/([sulphate] + [SO_2]). This choice was motivated by the fact, that most of the SO_2 at a later stage will be converted to sulphate. In fact, a test of the effect of running the model for a 7 days period showed that the [MSA]/[nss-sulphate] ratio after 7 days deviated less than 5% from the [MSA]/([sulphate] + [SO_2]) ratio after 24 hours.

4.1. SIMULATIONS FOR DRY AND GENERAL (NON DRY) CONDITIONS

Simulations of the updated KIM model have been carried out at several latitudes in both dry and non dry conditions, i.e., switching on and off the multiphase chemistry (see Table II). The model outcomes have then been compared with the observational data reported in Bates *et al.* (1992). Various options and model schemes have been tested against the data, especially for the mechanism of the liquid phase chemistry reaction. The final results and data are shown in the Figure 6, where data from Bates *et al.* (1992) – with their uncertainty bars – are compared against the averages obtained in the MC simulations, plotted with their Standard Deviation bars. The error bars representing the uncertainty in the observational data are chosen to be $\pm 6.5\%$ on the basis of the R^2 value given in Bates *et al.*. (1992). For each of the latitudes under consideration, model predictions are close in magnitude to the observed data. Given the large number of parameters involved in the DMS oxidation patterns and their uncertainty, the results obtained can be considered as a positive corroboration of the proposed mechanism.

Also note that results confirmed the importance of the introduction of the multiphase chemistry into the KIM model. The values of the MSA/(SO_2 + H_2SO_4) ratio predicted by KIM in dry conditions (i.e., when only the homogeneous chemistry was considered), were in magnitude far away from observational data (Figure 6). The agreement between model predictions and observational data has

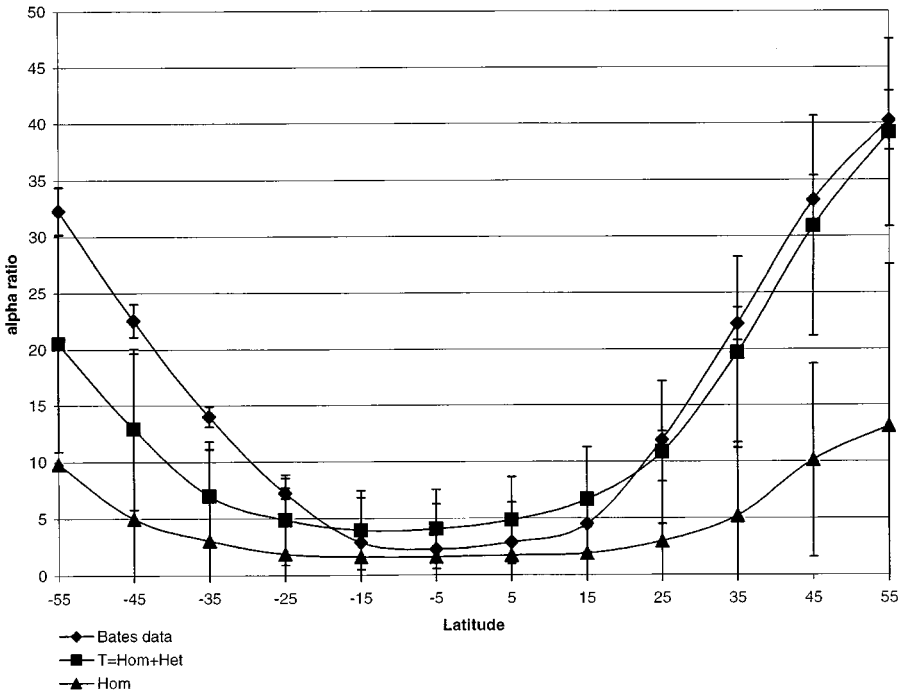

Figure 6. The KIM model predictions for the ratio [MSA/nss-SO_4^{2-}] are compared with the observational data reported in Bates *et al.* (1992). The model outcomes are plotted as averages obtained in the MC simulations, with their Standard Deviation bars, at several latitudes (winter scenario). The error bars representing the uncertainty in the observational data are chosen to be $\pm 6.5\%$ on the basis of the R^2 value given in Bates *et al.* (1992). The value assumed for k_{21} is the one found by Ray *et al.* (1996).

been significantly improved by the addition of the multiphase chemistry to the system.

4.2. SENSITIVITY ANALYSIS ON KIM (WITH AND WITHOUT MULTIPHASE CHEMISTRY)

As a consequence of the developments described in the previous sections, several kinetic constants have been added into KIM. Thus, at present, the model involves 68 input variables (see Table I in Appendix A). It follows that, with such a large number of variables, any SA measure based on a regression (SRC, PCC, etc.) can not be trusted with any reasonable level of confidence (Draper and Smith, 1981).

In order to perform the SA on KIM focusing only on a limited number of variables, a preliminary analysis has been conducted and the 20 most influential input variables (out of the total 68 contained in KIM) have been identified. The preliminary analysis has been carried out as follows:

1. the PREP pre-processor has been executed ten times, each time using a different seed for the random numbers generator;
2. on each of the ten sets of input variables generated by PREP, the KIM model has been run in a Monte Carlo fashion (number of runs = 100);
3. for each of the Monte Carlo performance, the 10 most important input variables have been identified by SPOP;
4. the input variables which have been recognised (i.e., which resulted to be included among the 10 most important) at least three times (out of the ten MC analysis executed) have been selected for further analysis.

The following input variables were identified:

$DEHDMSO_2$	$RHLH_2O_2$	W_{10}	k_{13}
$DEHH_2O_2$	$RHLNH_3$	WATLIQ	k_{15}
$DEHHNO_3$	$RHLO_3$	Q_1	k_{18}
DEHMSA	RHLDMS	Q_{21}	Q_{21}
$DEHO_3$	RHLDMSO	QW_7	k_{34}

Among those variables, the diffusion coefficients (DEH ...), the Henry's law constants (RHL ...), the water liquid content (WATLIQ) and the constant k_{18} (contained in the reaction $CH_3SOCH_3 + OH$), are involved in the heterogeneous chemistry part of the model (see Appendix A, Table I). The other variables are involved in the reactions explaining the homogenous chemistry.

The input variables not included among the twenty cited above, have been fixed to their 'nominal' value and kept constant through the succeeding KIM simulations. The 'nominal' value is chosen to be the mean of the statistical distribution adopted in PREP for sampling the variable.

SA (on the twenty variables) has been performed firstly, considering only the homogeneous part of the KIM model, and secondly, on the whole model (i.e., including also the heterogeneous chemistry). Three different latitudes (+35, –5, –55) have been taken into consideration in order to examine the dependency on latitude of the DMS oxidation pathways.

A Monte Carlo type sensitivity analysis has been chosen: the model has been run in a Monte Carlo fashion on a number of 1000 sets of input variables generated by the PREP subroutine (Section 3.1). Then, the SRC regression coefficients (Iman *et al.*, 1981), have been computed from the least-square regression analysis applied to the Monte Carlo simulation (by using the SPOP subroutine described in Section 3.1). When the regression is effective, the parameter influence can be assessed based on the absolute values of the SRC. The significance of the SRC coefficients has been tested by using the t-Student statistical test (Conover, 1980).

The effectiviness of the regression has also been measured by computing the model determination coefficient, R^2. For each of the three latitudes, and in both cases (with/without inclusion of heterogeneous chemistry), the R^2 coefficient was

in the range [0.7–0.8]. Values in that range can be regarded as an indication of a good fit of the model into data.

Results, given in Table III, indicate which are the most important parameter uncertainties with respect to the output variable (the ratio MSA/($SO_2+H_2SO_4$), in the following called α). The results for the three latitudes that have been investigated (Table III) show that the uncertainties related to the rate constants of the gas phase reactions [1], $CH_3SCH_3 + OH \rightarrow CH_3S\cdot$, and [21], $CH_3S(O)_2\cdot \rightarrow CH_3\cdot + SO_2$, in all cases remain the most important.

In the case of homogeneous gas phase chemistry only, the four highest ranking uncertainties are the same at all of the three latitudes.

The most important uncertainty is that on Q_1 (the quantile of k_1), and then, consequently, on the branching ratio between OH-radical addition and hydrogen-abstraction in the reaction between OH and DMS (in the following called β). A negative dependence of α on k_1 is found, showing that the addition pathway also in the homogeneous gas phase chemistry case favours the formation of MSA. This can be understood by inspection of the reaction scheme in Figure 1, showing that the reactions competing with formation of MSA are of more relevance in the hydrogen-abstraction pathway than in the alternative pathway.

k_{21} is important for the already mentioned reasons. The value of the rate constant for the hypothetical Reaction [34], $CH_3S(O)CH_3+OH \rightarrow (a)\, CH_3S(O)_2CH_3+ (1-a)\, CH_3S(O)\cdot$, which has been attributed a high uncertainty, is relevant because it controls the gas phase yield of $DMSO_2$ (which subsequently can form MSA) from the oxidation of DMSO.

Reaction [13], $CH_3SO\cdot + NO_2 \rightarrow CH_3 + SO_2\cdot + NO$, is a reaction competing with the gas phase formation of MSA; it is a hypothetical reaction which is highlighted in the statistical analysis because of the high uncertainty attributed to k_{13}.

When the aqueous phase chemistry is included, the value of k_1 remains a very important parameter, even more important than in the case of homogeneous gas phase chemistry only. This is not surprising since the OH addition pathway becomes even more favourable for the formation of MSA in this case since now also the aqueous phase chemistry contributes to the conversion of DMSO and $DMSO_2$ to MSA.

The high ranking of k_{21} must be explained by the large uncertainty attributed to this value. In fact the actual contribution of the gas phase pathway to MSA formation is rather small, as can be seen in Table II by comparing the values of α found in the case with gas phase chemistry to that of the multiphase system.

Reaction [34], $CH_3S(O)CH_3 + OH \rightarrow (a)\, CH_3S(O)_2CH_3 + (1-a)\, CH_3S(O)\cdot$, is still important for the before-mentioned reasons: it influences the formation of MSA by controlling the gas phase yield of $DMSO_2$ ($DMSO_2$ form MSA from the oxidation of DMSO).

For the heterogeneous chemistry case, also important are the Henry's law coefficients controlling the availability of the oxidants O_3 and H_2O_2 in the aqueous

phase, which are relevant uncertainties at the higher temperatures but not at –55 degree latitude. At –55 degree latitude none of the Henry's law coefficients seem important, possibly because the equilibria are shifted so much towards the aqueous solution that the uncertainties become irrelevant. Among the aqueous phase reactions only the uncertainty on the value of k_{w7} was found to be of significant importance. The significance of this reaction, which is $CH_3SCH_3 + O_3 \rightarrow CH_3S(O)CH_3$, must be explained by the fact that oxidation of DMS to DMSO (and further on to MSA) competes with the evaporation of DMS from the aqueous solution.

At the tropical latitude (–5 degrees) also the uncertainty of the Henry's law coefficient for DMS is of importance while the uncertainty on this parameter is not considered as being important at the other latitudes. However, this observation should not lead to the conclusion that the aqueous phase oxidation of DMS would be unimportant at other latitudes. In fact, if the model is run without including the transfer of DMS to the aqueous phase in the +35 degree latitude winter scenario, α is reduced from 19.70% to 5.16%.

Though most of the present discussion has dealt with parametric uncertainties, structural uncertainty should not be forgotten. The stochastic agreement between model predictions and observations has to be considered as a corroboration of the proposed mechanism (in the sense of Oreskes *et al.*, 1994). Other mechanisms could be put forward; particularly the parameterisation of the liquid phase chemistry has a high degree of structural uncertainty. With this important caveat, and based on the results of the present numerical experiment, we speculate that the contribution to formation of MSA by the aqueous phase chemistry of DMS, DMSO and $DMSO_2$ could possibly explain the observed temperature dependency of α.

5. Changing the k_{21} Value

Results of the present exercise have highlighted the fundamental role of the multiphase chemistry in explaining the latitude dependency of the ratio α observed by Bates *et al.* (1992) (Section 4.1). Among other things, the heterogeneous chemistry scheme conjectured here, depends on the value chosen for the kinetic constant k_{21}. In fact, a change in the value assumed for k_{21} would consequently result in a change of the pathways hypothesised for the liquid phase chemistry. Further, the sensitivity analysis exercise has underscored the strong sensitivity of the model on the value of k_{21}. Thus, the choice of the k_{21} value plays a key role in the present modelling attempt.

Unfortunately, estimates of the k_{21} value presented in the literature show strong discrepancies (for a review see Saltelli and Hjorth, 1995), and, still at present, this value is subject of an intense debate. In this work, the value assumed for k_{21} is the one found, in a very recent study, by Ray *et al.* (1996). However, given the recognised importance of this factor, we feel appropriate to explore the outcomes – both in terms of model structure and system behaviour – deriving from an alternative

choice for the k_{21} value. This choice is also justified by the fact, that the value of k_{21} determined by Ray *et al.* (1996) is much higher than what could be estimated from the endothermicity of the reaction assuming pre-exponential factors of 10^{13} or 10^{14}: for a ΔH of 21 kcal/mole (DeMore *et al.*, 1994) this calculation gives values of k_{21} in the range between 4×10^{-3} to 4×10^{-2} s^{-1} at 298 K. If in stead the activation energy of 18 kcal (Benson, 1978, and adopted in the present model) is applied with the same pre-exponential factors, then k_{21}-values between 6.6×10^{-1} and 6.6 s^{-1} are found, thus in both cases well below the value found by Ray *et al.* of 510 s^{-1}.

In this section, the distribution function assumed for k_{21} in Section 3.3, is replaced with the one already used by Saltelli and Hjorth (1995). The kinetic constant k_{21} is assumed to follow a uniform distribution between two temperature dependent bounds. For a certain temperature T, the bounds are computed as

$$UB_T = 1.e13 \exp \frac{UE_{298}}{RT}$$

$$LB_T = 1.e13 \exp \frac{LE_{298}}{RT}$$

with $UE_{298} = -16.5$ Kcal and $LE_{298} = -22.4$ Kcal.

The multiphase chemistry scheme presented in Figure 2, is now modified on the basis of the new value assumed for k_{21}. The structure of the scheme and its pathways are maintained unvaried, but the percentages of the fluxes numbered 11, 13 and 14, are estimated again. By using the same calibration procedure as in Section 3.4, the following percentages are obtained:

- 78.5% for the path going from $DMSO_2$ to SO_4^{2-};
- 21.5% for the path going from $DMSO_2$ to MSA.

Results of the simulations obtained by deriving the k_{21} value from the new distribution are reported in Table IV. Results are also displayed in Figure 7, where the averages of the MC simulations are plotted with error bars assumed equal to the Standard Deviations. The observational data from Bates *et al.* (1992) are also plotted for comparison with their error bars.

When using the k_{21} value proposed by Ray *et al.* (1996), a very good agreement was obtained between model predictions and observed data, both in terms of trend and magnitude (Figure 6). When using the new k_{21} value, this high level of agreement is no longer achieved. Under the new assumptions, the simulated data do not reproduce the trend of the experimental values (Figure 7), while under the old assumptions (Figure 6), model predictions were quite well representing the experimentally observed latitude dependency of α. Thus, in the case where the formation rate of MSA is strongly influenced by aqueous phase chemistry, the agreement with the experimental data is much better than in the case where gas phase reactions are

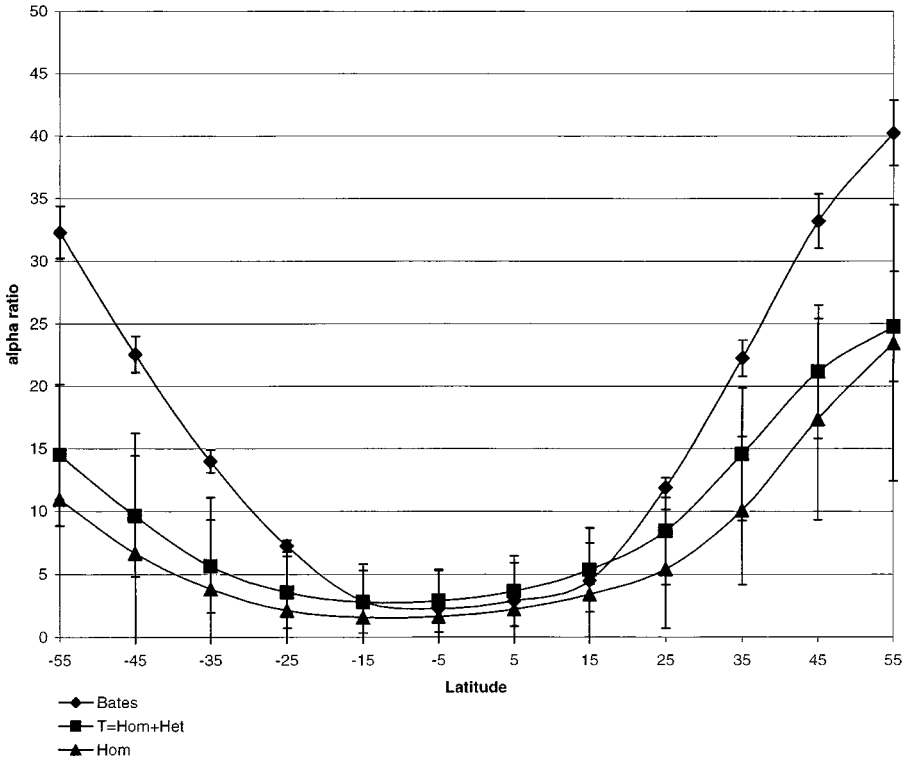

Figure 7. The KIM model predictions for the ratio alpha are compared with the observational data reported in Bates *et al.* (1992). The model outcomes are plotted as averages obtained in the MC simulations, with their Standard Deviation bars, at several latitudes (winter scenario). The error bars representing the uncertainty in the observational data are chosen to be $\pm 6.5\%$ on the basis of the R^2 value given in Bates *et al.* (1992). The value assumed for k_{21} is the one found in Saltelli and Hjorth, 1995.

more influential. This suggests that the temperature dependencies related to the multiphase chemistry (e.g., that of the Henry's law constants) could be the main factor controlling the temperature dependencies of α.

6. Conclusions

Two main conclusions can be drawn from our modelling exercise. The first one is that, to reproduce the observed latitudinal distribution of the ratio α, the model must simulate the multi-phase tropospheric chemistry. A model considering only the gas-phase chemistry does not perform properly (in the sense that its predictions are not corroborated from experimental data). The second is that, in order to conduct successfully the modelling exercise, an accurate estimate of the kinetic constant k_{21} of the model is needed. This has been proved by both the SA exercise (Section 4.2), which has recognised k_{21} as one of the most influential factor in the

model, and the study conducted in Section 5, which has shown how the model outcomes are heavily depending on the choice of the distribution for k_{21}.

Results have also shown that, if the value of k_{21} found by the most recent and most direct study (Ray *et al.*, 1996) is correct, then little MSA will be formed through reactions involving the CH_3SO_2 radical because this intermediate will rapidly dissociate. Other explanations for the α values observed experimentally must then be sought, either via pure gas phase reaction pathways or via pathways involving liquid phase chemistry as well.

Koga and Tanaka (1993) have suggested that the OH-DMS adduct could form MSA by reaction with O_2 through a sequence of fast reaction steps. However, this would give α the same temperature dependence as that of the branching ratio β and, as pointed out by Barone *et al.* (1995), this is different from what observed.

The results of the present study show that multi-phase tropospheric chemistry could explain the actually observed latitudinal distribution of α in the troposphere (Figures 6 and 7). Our hypothesised reaction scheme proceeds via the formation of DMSO from the initial OH-DMS adduct, which then is further oxidised to MSA in the aqueous phase. The most important pathway, however, is the one starting with absorption of DMS on water droplets followed by its stepwise oxidation to MSA. As a result, the temperature dependence of α will be determined by the temperature dependence of β, as well as by the temperature dependencies of the other gas phase/aqueous phase equilibria. It must be kept in mind that the results of this exercise depend much on the choice of the reaction mechanism, in particular the assumptions about the fate of DMS dissolved in water droplets.

Acknowledgements

This work has been partially funded by the European Commission programme INTAS, contract INTAS-RFBR 95-0726, on Stochastic modelling, and by the European Commission, DGXII, within the contract ENV4-CT97-0410 ‘DOMAC’.

Appendix A

Table I. Data for the model. Gas phase and liquid phase reaction rate constants, Henry’s law constants and their temperature dependence. Reactions [1] to [36] are gas phase reactions, reactions [w1] to [w15] are liquid phase reactions, and reactions [H1] to [H10] are Henry’s law constants

Reactions		$k_{298\,K}$ (cm^3 $molecule^{-1}$ s^{-1}, unless other stated)	$f_{298\,K}$	A (cm^3 $molecule^{-1}$ s^{-1}, unless other stated)	$E/R \pm (\Delta E/R)$ (K)	Refs. and comments
Gas phase reactions:						
[1]	$CH_3SCH_3 + OH \rightarrow CH_3S\cdot$	5.0×10^{-12}	1.20	1.1×10^{-11}	240 ± 100	[R1], [R2] [R3], [R4] C1

Table I. (Continued)

Reactions		$k_{298\ K}$ (cm^3 $molecule^{-1}$ s^{-1}, unless other stated)	$f_{298\ K}$	A (cm^3 $molecule^{-1}$ s^{-1}, unless other stated)	$E/R \pm (\Delta E/R)$ (K)	Refs. and comments
[2]	$CH_3SCH_3 + OH \rightarrow CH_3S(OH)CH_3$	1.1×10^{-12}	1.71	–	–	[R1], [R2] C2
[3]	$CH_3S(OH)CH_3 + O_2 \rightarrow CH_3SO\cdot$	2.0×10^{-12}	1	–	–	[R5], [R6] C3
[5]	$CH_3S + NO_2 \rightarrow CH_3SO\cdot + NO$	6.0×10^{-11}	1.21	$(2.06 \pm 0.44) \times 10^{-11}$	-320 ± 40	[R7], [R8] C5
[6]	$CH_3S + O_3 \rightarrow CH_3SO\cdot + O_2$	5.2×10^{-12}	1.19	$(1.98 \pm 0.38) \times 10^{-12}$	-290 ± 40	[R7] C6
[7]	$CH_3S + O_2 \rightarrow CH_3SOO\cdot$	1.5×10^{-19}	a	–	–	[R8], [R9], [R10], C7
[–7]	$CH_3SOO\cdot \rightarrow CH_3S + O_2$	$1\ s^{-1}$	a	–	–	[R8], [R9], [R10], C7
[8]	$CH_3SOO\cdot \rightarrow CH_3S(O)_2\cdot$	$1\ s^{-1}$	a	–	–	[R7], [R11], C8
[9]	$CH_3SOO\cdot + NO \rightarrow CH_3SO\cdot + NO_2$	1.1×10^{-11}	1.40	–	–	[R7] C9
[10]	$CH_3SO + O_3 \rightarrow CH_3SO_2\cdot + O_2$	3.0×10^{-13}	a	–	–	[R12] C10
[11]	$CH_3SO + O_3 \rightarrow CH_3 + SO_2 + O_2$	3.0×10^{-13}	a	–	–	[R12] C11
[12]	$CH_3SO\cdot + NO_2 \rightarrow CH_3SO_2\cdot + NO$	1.2×10^{-11}	1.30	–	–	[R13], [R14] [R15], [R16] C12
[13]	$CH_3SO\cdot + NO_2 \rightarrow CH_3 + SO_2\cdot + NO$	1.8×10^{-12}	a	–	–	[R11] C13
[14]	$CH_3S(O)\cdot + O_2 \rightarrow CH_3S(O)O_2\cdot$	7.7×10^{-18}	a	–	–	[3], [4] C14
[-14]	$CH_3S(O)O_2\cdot \rightarrow CH_3S(O)\cdot + O_2$	$170\ s^{-1}$	a	–	–	[3], [4], [R17], C14
[15]	$CH_3S(O)O_2\cdot + NO_2 \rightarrow CH_3S(O)O_2\ NO_2$	5.89×10^{-12}	a	–	–	[R10], [3], [4], C15
[–15]	$CH_3S(O)O_2\ NO_2 \rightarrow CH_3S(O)O_2\cdot + NO_2$	$0.7\ s^{-1}$	a	–	–	[R10], [R11], [R18], C15
[16]	$CH_3S(O)O_2\cdot + NO \rightarrow CH_3S(O)O\cdot + NO_2$	1.0×10^{-11}	a	–	–	[R10], [3], [4], [R7], C16
[17]	$CH_3S(O)_2\cdot + NO_2 \rightarrow CH_3S(O)_2O\cdot + NO$	2.2×10^{-12}	1.50	–	–	[R19] C17
[18]	$CH_3S(O)_2\cdot + O_3 \rightarrow CH_3S(O)_2O\cdot + O_2$	6.3×10^{-13}	a	–	–	[R11], C18
[19]	$CH_3S(O)_2\cdot + O_2 \rightarrow CH_3S(O)_2O_2\cdot$	2.6×10^{-18}	a	–	–	[3], [4] [R17], C19
[–19]	$CH_3S(O)_2O_2\cdot \rightarrow CH_3S(O)_2\cdot + O_2$	$170\ s^{-1}$	a	–	–	[3], [4], [R17], C19
[20]	$CH_3S(O)_2O_2\cdot + NO_2 \rightarrow CH_3S(O)_2O_2\ NO_2$	5.89×10^{-12}	a	–	–	[R10], [3], [4], C20
[–20]	$CH_3S(O)_2O_2\ NO_2 \rightarrow CH_3S(O)_2O_2\cdot + NO_2$	$0.0115\ s^{-1}$	a	–	–	[R10], [R11], [R18], C20
[21]	$CH_3S(O)_2\cdot \rightarrow CH_3\cdot + SO_2$	$510\ s^{-1}$	1.59	–	–	[R19], C21
[22]	$CH_3S(O)_2O\cdot \rightarrow CH_3\cdot + SO_3$	$0.0012\ s^{-1}$	a	–	–	[R11], C22
[23]	$CH_3S(O)_2O\cdot \rightarrow CH_3SO_3H$	$5.0\ s^{-1}$	a	–	–	[R11], C23
[25]	$SO_2 + OH \rightarrow H_2SO_4$	2.0×10^{-12}	a	–	–	[R10], [R11] C25
[26]	$CH_3S(O)_2O_2\cdot + NO \rightarrow CH_3S(O)_2O\cdot + NO_2$	1.0×10^{-11}	a	–	–	[R10], [3], [4], [R7], C26

Table I. (Continued)

Reactions		$k_{298\ K}$ (cm^3 $molecule^{-1}$ s^{-1}, unless other stated)	$f_{298\ K}$	A (cm^3 $molecule^{-1}$ s^{-1}, unless other stated)	$E/R \pm (\Delta E/R)$ (K)	Refs. and comments
[28]	$CH_3SOO\cdot + NO_2 \rightarrow CH_3SOONO_2$	2.2×10^{-11}	1.27	–	–	[R10], [3], [4], [R7], C28
[–28]	$CH_3SOONO_2 \rightarrow CH_3SOO\cdot + NO_2$	$0.7\ s^{-1}$	a	–	–	[R10], [R11], C28
[29]	$CH_3SOO\cdot + O_3 \rightarrow CH_3SO\cdot + 2\,O_2$	4.0×10^{-13}	a	–	–	[R7], [R12] C29
[30]	$CH_3S\cdot + O_2 \rightarrow CH_3\cdot + SO_2$	3.0×10^{-18}	a	–	–	[R8], [R20] C30
[31]	$CH_3SOO\cdot + O_2 \rightarrow CH_3\cdot + SO_2$	2.0×10^{-17}	a	–	–	[R8], [R20] C31
[33]	$CH_3S(OH)CH_3 + O_2 \rightarrow CH_3S(O)CH_3$	2.0×10^{-12} 1	–	–	[R6]	C33
[34]	$CH_3S(O)CH_3 + OH \rightarrow$ (a) $CH_3S(O)_2CH_3 +$ (1-a) $CH_3S(O)\cdot$	6.22×10^{-11}	1.35	–	–	[R5] C34
[36]	$CH_3S(O)_2CH_3 + OH \rightarrow CH_3S(O)_2\cdot$	2.5×10^{-13}	a	–	–	[R18] C36
Liquid phase reactions:						
[w1]	$SO_2 + O_3 \rightarrow H_2SO_4$	$2.4 \times 10^4\ M^{-1}\ s^{-1}$	1	–	–	[R21] Cw1
[w2]	$HSO_3^- + O_3 \rightarrow H_2SO_4$	$3.7 \times 10^5\ M^{-1}\ s^{-1}$	1	4.24×10^{13}	5530	[R21], [R22] Cw2
[w3]	$SO_3^{2-} + O_3 \rightarrow H_2SO_4$	$1.5 \times 10^9\ M^{-1}\ s^{-1}$ Cw3	1	7.43×10^{13}	5280	[R21], [R22]
[w4]	$HSO_3^- + H_2O_2 \rightarrow H_2SO_4$	a	a	a	a	[R21], [R23], Cw4
[w6]	$CH_3SCH_3 + H_2O_2 \rightarrow CH_3S(O)CH_3$	$3.4 \times 10^{-2}\ M^{-1}\ s^{-1}$	1	–	–	[R24] Cw6
[w7]	$CH_3SCH_3 + O_3 \rightarrow CH_3S(O)CH_3$	$6.1 \times 10^8\ M^{-1}\ s^{-1}$	1.40	$6.7 \times 10^{15}\ M^{-1}\ s^{-1}$	4831 ± 1000	[R25] Cw7
[w8]	$CH_3S(O)CH_3 + O_3 \rightarrow CH_3S(O)_2CH_3$	$5.7\ M^{-1}\ s^{-1}$	1.04	–	–	[R25] Cw8
[w9]	$CH_3SCH_3 + OH \rightarrow CH_3S(O)CH_3$	$5.2 \times 10^9\ M^{-1}\ s^{-1}$	1	–	–	[R26] Cw9
[w10]	$CH_3S(O)CH_3 + OH \rightarrow CH_3S(O)_2CH_3$	$5.4 \times 10^9\ M^{-1}\ s^{-1}$	1.06	–	–	[R27] Cw10
[w11]	$CH_3S(O)_2CH_3 + OH \rightarrow H_2SO_4 + MSA$	$2.7 \times 10^7\ M^{-1}\ s^{-1}$	1.06	–	–	[R27] Cw11
[w12]	$CH_3S(O)CH_3 + H_2O_2 \rightarrow CH_3S(O)_2CH_3$	$3.4 \times 10^{-2}\ M^{-1}\ s^{-1}$	1	–	–	[R24] Cw12
[w13]	$CH_3S(O)_2CH_3 + H_2O_2 \rightarrow H_2SO_4 + MSA$	$3.4 \times 10^{-2}\ M^{-1}\ s^{-1}$	1	–	–	[R24] Cw13
[w14]	$CH_3S(O)_2CH_3 + O_3 \rightarrow H_2SO_4$+ MSA	$5.7\ M^{-1}\ s^{-1}$	1.04	–	–	[R25] Cw14
[w15]	$CH_3S(O)_2OH + OH \rightarrow H_2SO_4$	$3.0 \times 10^7\ M^{-1}\ s^{-1}$	1.40	–	–	[R27], [R28], Cw15
Henry's law constants:						
[H1]	$H(CO_2)$	$3.4 \times 10^{-2}\ M\ atm^{-1}$	1.20	–	2439 ± 489	[R29], Ch1
[H2]	$H(SO_2)$	$1.24\ M\ atm^{-1}$	1.20	–	3144 ± 629	[R29], Ch1

Table I. (Continued)

Reactions		$k_{298\,K}$ (cm^3 $molecule^{-1}$ s^{-1}, unless other stated)	$f_{298\,K}$	A (cm^3 $molecule^{-1}$ s^{-1}, unless other stated)	$E/R \pm (\Delta E/R)$ (K)	Refs. and comments
[H3]	$H(NH_3)$	62 M atm^{-1}	1.20	–	4112 ± 822	[R29], Ch1
[H4]	$H(H_2O_2)$	7×10^4 M atm^{-1}	1.20	–	7297 ± 1459	[R29], Ch1
[H5]	$H(O_3)$	9.4×10^{-3} M atm^{-1}	1.20	–	2536 ± 507	[R29], Ch1
[H6]	$H(CH_3SCH_3)$	0.56 M atm^{-1}	1.20	–	4479 ± 896	[R30], [R31], Ch1
[H7]	$H(CH_3S(O)CH_3)$	1.0×10^7 M atm^{-1}	1.50	–	2577 ± 515	[R32], [R25], [R33], Ch7, Ch1
[H8]	$H(CH_3S(O)_2CH_3)$	1.0×10^7 M atm^{-1}	1.50	–	5385 ± 1077	[R32], [R25], [R33], Ch8 Ch1
[H9]	$H(CH_3SO_3H)$	1.0×10^9 M atm^{-1}	1.50	–	1761 ± 352	[R33], [R34], Ch9, Ch1
[H10]	$H(H_2SO_4)$	Infinity	–	–	–	Ch10

[a] See under comments.

$k_T = A\exp\{-E/RT)\}$, Arrhenius expression.

A = Pre-exponential factor A, unit = cm^3 $molecule^{-1}$ s^{-1}.

E = Activation energy, unit = J $mole^{-1}$ = L atm $mole^{-1}$.

R = Gas constant. = 8.314 J K^{-1} $mole^{-1}$ = 0.08206 L atm K^{-1} $mole^{-1}$ = 1.987 cal K^{-1} $mole^{-1}$.

f = Uncertainty of k.

$f_{298\,K}$ = Uncertainty of k at 298 K.

f_T = Estimate of the uncertainty k_T at temperature T.

$f_T = f_{298\,K}\exp\{|\Delta E/R(T^{-1} - (298\,K)^{-1})|\}$.

ΔE = Uncertainty in the activation energy, unit = J $mole^{-1}$.

Comments:

C1: Normal distribution with average k_1 and uncertainty f_1.

C2: $k_2 = \{\{T\exp(-234/T) + 8.46\times10^{-10}\exp(7230/T) + 2.68\times10^{-10}\exp(7810/T)\}/\{1.04\times10^{11}T + 88.1\exp(7460/T)\}\} - k_1$ as recommended in R10. Uniform distribution with average k_2 and uncertainty f_2.

C3: Constant and assumed to be independent of temperature. C5: Normal distribution with average k_5 and uncertainty f_5.

C6: Normal distribution with average k_6 and uncertainty f_6.

C7: $K_7 = k_7(k_{-7})^{-1}$. In this investigation we set $k_7 = K_7$ and $k_{-7} = 1$ s^{-1}. k_7 is lognormal distributed with $k_7 = \exp(\Delta S/R)\exp(-\Delta H/(RT))1.36 \times 10^{-22}T$, where $\Delta S = -32.2$ cal K^{-1} mol^{-1}, $\Delta H = -10400$ cal mol^{-1} and $1.36 \times 10^{-22}T$ is the transformation factor from K_p into K_c as explained in Ref. 71. k_7 is obtained from the two equations: $\Delta G = \Delta H - T\Delta S$ and $\Delta G = -RT\ln K_p$. With uncertainty $f_T = \sigma(A) = \sigma(\Delta S/R) = \ln\{4.1\exp\{800$ cal mol^{-1} R^{-1} $(T^{-1} - (298\,K)^{-1})\}\}R$ and $\sigma(\Delta H) = 800$ cal mol^{-1}.

C8: Lognormal distribution between $10^{-0.29}$ and $10^{0.31}$, with average $10^{0.01}$. Assumed to be independent of temperature.

C9: Normal distribution with average k_9 and uncertainty f_9 and assumed to be independent of temperature.

C10: Uniform distribution between 0 and 6.0×10^{-13} cm^3 $molecule^{-1}$ s^{-1}. Assumed to be independent of temperature.

C11: Uniform distribution between 0 and 6.0×10^{-13} cm^3 $molecule^{-1}$ s^{-1}. Assumed to be independent of temperature.

C12: Normal distribution with average k_{12} and uncertainty f_{12}. Assumed to be independent of temperature.

C13: Uniform distribution between 0 and 3.6×10^{-12} cm^3 $molecule^{-1}$ s^{-1}. Assumed to be independent of temperature.

C14: k_{14} is uniform distributed between 7.7×10^{-19} cm^3 $molecule^{-1}$ s^{-1} and 7.7×10^{-17} cm^3 $molecule^{-1}$ s^{-1}. Assumed to be independent of temperature. k_{-14} is lognormal distributed between 17 s^{-1} and 1700 s^{-1}, with average 170 s^{-1}. As a function of temperature: $k_{-14}(T) = A\exp(B/(RT))$, where $A = 3.0 \times 10^{11}$ s^{-1} and $B = \Delta H = -12500$ cal mol^{-1} with uncertainty $f_T = 10\exp\{2000$ cal mol^{-1} $R^{-1}|(T^{-1} - (298\,K)^{-1})|\}\}$ and $\sigma(B) = 2000$ cal mol^{-1}, $k_{-14}(T)$ is lognormal distributed with average $\log_{10}(k_{-14}(T))$ and uncertainty $\log_{10}(f_T)$.

C15: k_{15} is lognormal distributed between $10^{-11.73}$ and $10^{-10.73}$, with average $10^{-11.23}$. Assumed to be independent of temperature. k_{-15} is lognormal distributed between 0.04 s^{-1} and 12 s^{-1}, with average 0.7 s^{-1}. As a function of temperature: $k_{-15}(T) = A\exp(B/(RT))$, where $A = 1.1 \times 10^{10}$ s^{-1} and $B = \Delta H = -13900$ cal mol^{-1} with uncertainty $f_T = 17\exp\{4000$ cal mol^{-1} $R^{-1}|(T^{-1} - (298\,K)^{-1})|\}\}$ and $\sigma(B) = 4000$ cal mol^{-1}, $k_{-15}(T)$ is lognormal distributed with average $\log_{10}(k_{-15}(T))$ and uncertainty $\log_{10}(f_T)$.

C16: Lognormal distribution between $10^{-11.3}$ and $10^{-10.7}$, with average 10^{-11}. Assumed to be independent of temperature.

C17: Uniform distribution with average k_{17} and uncertainty f_{17}. Assumed to be independent of temperature.

C18: Lognormal distribution between $10^{-12.72}$ and $10^{-11.72}$ with average $10^{-12.22}$. Assumed to be independent of temperature. C19: k_{19} is uniform distributed between 2.6×10^{-20} cm^3 $molecule^{-1}$ s^{-1} and 2.6×10^{-16} cm^3 $molecule^{-1}$ s^{-1}. Assumed to be independent of temperature. k_{-19} is lognormal distributed between 17 s^{-1} and 1700 s^{-1}, with average 170 s^{-1}. As a function of temperature: $k_{-19}(T) = A\exp(B/(RT))$, where $A = 3.0 \times 10^{11}$ s^{-1} and $B = \Delta H = -12500$ cal mol^{-1} with uncertainty $f_T = 10\exp\{2000$ cal mol^{-1} $R^{-1}|(T^{-1} - (298\,K)^{-1})|\}\}$ and $\sigma(B) = 2000$ cal mol^{-1}, $k_{-19}(T)$ is lognormal distributed with average $\log_{10}(k_{-19}(T))$ and uncertainty $\log_{10}(f_T)$.

Table I. (Continued)

C20: k_{20} is lognormal distributed between $10^{-11.73}$ and $10^{-10.73}$, with average $10^{-11.23}$. Assumed to be independent of temperature. k_{-20} is lognormal distributed between 0.15 s^{-1} and 0.001 s^{-1}, with average 0.0115 s^{-1}. As a function of temperature: $k_{-20}(T) = A\exp(B/(RT))$, where $A = 1.8 \times 10^8$ s^{-1} and $B = \Delta H = -13900$ cal mol^{-1} with uncertainty $f_T = 17\exp\{2000$ cal mol^{-1} $R^{-1}|(T^{-1} - (298\text{ K})^{-1})|\}$ and $\sigma(B) = 2000$ cal mol^{-1}, $k_{-20}(T)$ is lognormal distributed with average $\log_{10}(k_{-20}(T))$ and uncertainty $\log_{10}(f_T)$.

C21: k_{21} is normal distributed. As a function of temperature: $k_{21}(T) = A\exp(B/(RT))$, where $A = 8.1 \times 10^{15}$ s^{-1} and $B = \Delta H = -18000$ cal mol^{-1} with uncertainty $f_T = 1.59\exp\{1510$ cal mol^{-1} $R^{-1}|(T^{-1} - (298\text{ K})^{-1})|\}\}$ and $\sigma(B) = 1510$ cal mol^{-1}, $k_{21}(T)$ is normal distributed with average $k_{-21}(T)$ and uncertainty f_T.

C22: Uniformly distributed between 2.4×10^{-3} s^{-1} and 1.1×10^{-7} s^{-1} at 298 K. As a funtion of temperature: $k_{22}(T)$ is uniformly distributed between $1 \times 10^{13}\exp(-21.3 \times 10^3 R^{-1}T^{-1})$ s^{-1} and $1 \times 10^{13}\exp(-27.2 \times 10^3 R^{-1}T^{-1})$ s^{-1}.

C23: Uniform distribution between 0.01 s^{-1} and 10 s^{-1}. Assumed to be independent of temperature.

C25: Uniform distribution between 1.0×10^{-12} cm^3 $molecule^{-1}$ s^{-1} and 3.0×10^{-12} cm^3 $molecule^{-1}$ s^{-1}. Assumed to be independent of temperature.

C26: Lognormal distribution between $10^{-11.3}$ and $10^{-10.7}$, with average 10^{-11}. Assumed to be independent of temperature.

C28: k_{28} is normal distributed with average k_{28} and uncertainty f_{28}. Assumed to be independent of temperature. k_{-28} is lognormal distributed between 0.04 s^{-1} and 12 s^{-1}, with average 0.7 s^{-1}. As a function of temperature: $k_{-28}(T) = A\exp(B/(RT))$, where $A = 1.1 \times 10^{10}$ s^{-1} and $B = \Delta H = -13900$ cal mol^{-1} with uncertainty $f_T = 17\exp\{4000$ cal mol^{-1} $R^{-1}|(T^{-1} - (298\text{ K})^{-1})|\}\}$ and $\sigma(B) = 4000$ cal mol^{-1}, $k_{-28}(T)$ is lognormal distributed with average $\log_{10}(k_{-28}(T))$ and uncertainty $\log_{10}(f_T)$.

C29: Uniform distribution between 0 and 8.0×10^{-13} cm^3 $molecule^{-1}$ s^{-1}. Assumed to be independent of temperature.

C30: Uniform distribution between 0 and 6.0×10^{-18} cm^3 $molecule^{-1}$ s^{-1}. Assumed to be independent of temperature.

C31: Uniform distribution between 0 and 6.0×10^{-18} cm^3 $molecule^{-1}$ s^{-1}. Assumed to be independent of temperature.

C32: Uniform distribution with average k_{32} and uncertainty f_{32}.

C33: Constant and assumed to be independent of temperature.

C34: Normal distribution with average k_{34} and uncertainty f_{34}. The factor a is also normal distributed with average 0.25 and uncertainty 0.07. Assumed to be independent of temperature. It should be mentioned that in a recent paper by Hynes and Wine (1996), is reported a slightly higher value of k_{34}, $(10 \pm 3) \times 10^{-11}$ cm^3 $molecule^{-1}$ s^{-1}, than the one suggested in this investigation.

C36: Uniform distribution between 0 and 5.0×10^{-13} cm^3 $molecule^{-1}$ s^{-1}. Assumed to be independent of temperature.

C37: Normal distribution with average k_{37} and uncertainty f_{37}. Assumed to be independent of temperature.

Cw1: Constant and assumed to be independent of temperature.

Cw2: Constant, but dependent of temperature.

Cw3: Constant, but dependent of temperature.

Cw4: $-d[HSO_3^-]/dt = k_{w4}\,[H^+]\,[H_2O_2]\,[HSO_3^-]\,(1 + k_{w5}[H^+])$ $k_{w4}(T) = 1.29 \times 10^{14}\exp(-4307T^{-1})$ M^{-1} s^{-1} $k_{w5} = 16$ M^{-1}

Cw6: Constant and assumed to be independent of temperature. The reaction product is assumed to be DMSO.

Cw7: $k_{w7}(T)$ is normal distributed with average $k_{w7}(T)$ and uncertainty f_T. The reaction product is assumed to be DMSO.

Cw8: k_{w8} is normal distributed with average k_{w8} and uncertainty f_{w8}. Assumed to be independent of temperature. The reaction product is assumed to be $DMSO_2$.

Cw9: Constant and assumed to be independent of temperature. The reaction product is assumed to be DMSO.

Cw10: k_{w10} is normal distributed with average k_{w10} and uncertainty f_{w11}. Assumed to be independent of temperature. The reaction product is assumed to be $DMSO_2$.

Cw11: k_{w11} is normal distributed with average k_{w11} and uncertainty f_{w11}. Assumed to be independent of temperature. The reaction products are assumed to be H_2SO_4 + MSA.

Cw12: Assumed to be similar to Reaction (w6). Constant and assumed to be independent of temperature. The reaction product is assumed to be $DMSO_2$.

Cw13: Assumed to be similar to Reaction (w6). Constant and assumed to be independent of temperature. The reaction products are assumed to be H_2SO_4 + MSA.

Cw14: Assumed to be similar to Reaction (w8). k_{w14} is normal distributed with average k_{w14} and uncertainty f_{w14}. Assumed to be independent of temperature. The reaction products are assumed to be H_2SO_4 + MSA.

Cw15: k_{w15} is normal distributed with average k_{w15} and uncertainty f_{w15}. Assumed to be independent of temperature. The reaction product is assumed to be H_2SO_4 in accordance with Saltzman *et al.* (1983).

Ch1: Henry law's const., k_{H1}, is normal distributed with average k_{H1} and uncertainty f_{H1}. Henry law's const. as a function of temperature: $k_{H1}(T)$ is calculated from the van't Hoff's equation (see ref. [R29]): $k_{H1}(T_2)\ (k_{H1}(T_1))^{-1} = \exp\{\Delta H R^{-1}(T_1^{-1} - T_2^{-1})\}$, where $\Delta H R^{-1} = -E/R$, which can be found in Table I. Uncertainty $f_{H1}(T) = f_{H1}\exp\{\Delta E$ cal mol^{-1} $R^{-1}|(T^{-1} - (298\text{ K})^{-1})|\}\}$, where $\Delta E R^{-1}$ can be found in Table I. $k_{H1}(T)$ is normal distributed with average $k_{H1}(T)$ and uncertainty factor $f_{H1}(T)$.

Ch7: Henry's law constant for $CH_3S(O)CH_3$ is assumed to be lower than the one from CH_3SO_3H. According to a recent paper by Lee and Zhou (1994), the Henry's law constant for DMSO is $> 1 \times 10^6$ M atm^{-1} and the Henry's law constant for DMSO has to be $< H_{MSA} = 1 \times 10^9$ M atm^{-1} (see under Ch9). By taking these two statements into consideration, we assumed a value of $H_{DMSO} = (1.0 \pm 0.5) \times 10^7$ M atm^{-1}, including a 50% uncertainty at 298 K.

Ch8: Henry's law constant for $CH_3S(O)_2CH_3$ is assumed to be similar to the one from $CH_3S(O)CH_3$. $DMSO_2$ is less polar than DMSO, but the boiling point for $DMSO_2$ is higher than the one for DMSO, indicating that the vapour pressure of DMSO is higher than for $DMSO_2$. In this investigation it was assumed that Henry's law constant for $DMSO_2$ is similar to the one of DMSO.

Ch9: Henry's law constant for CH_3SO_3H is assumed to be higher than 2×10^7 M atm^{-1}. According to Clegg and Brimblecombe (1985), the Henry's law constant for MSA is $> 2 \times 10^7$ M atm^{-1}. In this investigation we assumed a value of $H_{MSA} = (1.0 \pm 0.5) \times 10^9$ M atm^{-1}, including 50% uncertainty at 298 K.

Ch10: Henry's law constant for H_2SO_4 is assumed to inifinity large.

Table I. (Continued)

References:
[R1]: DeMore *et al.*, 1994.
[R2]: Hynes *et al.*, 1986.
[R3]: Yin *et al.*, 1990a.
[R4]: Yin *et al.*, 1990b.
[R5]: Barnes *et al.*, 1988.
[R6]: Koga and Tanaka, 1993.
[R7]: Turnipseed *et al.*, 1993.
[R8]: Turnipseed *et al.*, 1992.
[R9]: Barone *et al.*, 1995.
[R10]: Moore, 1978.
[R11]: Saltelli and Hjorth, 1995.
[R12]: Domine' *et al.*, 1992.
[R13]: Domine' *et al.*, 1990.
[R14]: Tyndall and Ravishankara, 1989.
[R15]: Mellouki *et al.*, 1988.
[R16]: Tyndall and Ravishankara, 1991.
[R17]: Benson, 1978.
[R18]: Falbe-Hansen *et al.*, 1998.
[R19]: Ray *et al.*, 1996.
[R20]: Turnipseed and Ravishankara, 1993.
[R21]: Seinfeld, 1986, pp. 218–229.
[R22]: Pandis and Seinfeld, 1989.
[R23]: McArdle and Hoffman, 1983.
[R24]: Adewuyi, 1989.
[R25]: Lee and Zhou, 1994.
[R26]: Betterton, 1992.
[R27]: Milne *et al.*, 1989.
[R28]: Olson and Fessenden, 1992.
[R29]: Seinfeld, 1986, pp. 198–201.
[R30]: Dacey *et al.*, 1984.
[R31]: Baulch *et al.*, 1982.
[R32]: Watts and Brimblecombe, 1987.
[R33]: De Bruyn *et al.*, 1994.
[R34]: Clegg and Brimblecombe, 1985.

Table II. Model predictions and observational values for the ratio MSA/($SO_2 + H_2SO_4$). The value used for k_{21} is taken from Ray *et al.* (1996). The model is run in two different conditions: (1) dry conditions, i.e., only the homogeneuos gas chemistry is considered; (2) general (non dry) conditions, i.e., multi-phase (homogeneous and heterogeneous) gas chemistry is simulated

Latitude	Model predictions in non dry conditions (multi-phase gas chemistry)	Model predictions in dry conditions (only homogeneous gas chemistry)	Observed values (Bates *et al.*, 1992)
–55	20.54%	9.8%	32.3%
–45	12.92%	4.99%	22.55%
–35	7%	3.05%	14%
–25	4.88%	1.87%	7.25%
–15	3.96%	1.61%	2.9%
–5	4.06%	1.6%	2.3%
5	4.83%	1.74%	2.9%
15	6.65%	1.91%	4.5%
25	10.83%	2.98%	11.9%
35	19.7%	5.21%	22.25%
45	30.91%	10.14%	33.2%
55	39.17%	13.12%	40.25%

Table III. Results of the SA on KIM at three different latitudes. The identified parameters are: Q1: the quantile for the distribution of k_1 in Reaction [1] of Table I; Q21: the quantile for the distribution of k_{21} in Reaction [21] of Table I; k_{34} in Reaction [34] of Table I; k_{13} in Reaction [34] of Table I; $RHLO_3$ the Henry's law constant for O_3 (in [H5] of Table I); $RHLH_2O_2$ the Henry's law constant for H_2O_2 (in [H4] of Table I); QW7, the quantile for the distribution of kW7 in reaction [W7] of Table I; RHLDMS, the Henry's law constant for DMS (in [H6] of Table I); k_{18}, in Reaction [18] of Table I; $DHLDMSO_2$, the diffusion coefficient of $DMSO_2$

Latitude	Most important variables (decreasing order) in the *Homogenous* chemistry part of the KIM model	Most important variables (decreasing order) in the KIM model (including *Homogeneous + Heterogeneous* chemistry)
+35	Q1	Q1
	Q21	Q21
	R34	$RHLO_3$
	R13	$RHLH_2O_2$
		QW7
		R34
–5	Q1	Q1
	Q21	Q21
	R34	QW7
	R13	$RHLO_3$
		RHLDMS
		R18
		$RHLH_2O_2$
		$DHLDMSO_2$
–55	Q1	Q1
	Q21	Q21
	R34	R34
	R13	QW7

Table IV. Model predictions and observational values for the ratio α. The value used for k_{21} is taken from Saltelli and Hjorth (1995). The model is run in two different conditions: (1) dry conditions, ie only the homogeneuos gas chemistry is considered; (2) general (non dry) conditions, i.e., multi-phase (homogeneous and heterogeneous) gas chemistry is simulated

Latitude	Model predictions in non dry conditions (multi-phase gas chemistry)	Model predictions in dry conditions (only homogeneous gas chemistry)	Observed values (Bates *et al.*, 1992)
–55	14.5%	10.94%	32.3%
–45	9.64%	6.67%	22.55%
–35	5.63%	3.83%	14%
–25	3.58%	2.12%	7.25%
–15	2.82%	1.6%	2.9%
–5	2.9%	1.65%	2.3%

Table IV. (Continued)

Latitude	Model predictions in non dry conditions (multi-phase gas chemistry)	Model predictions in dry conditions (only homogeneous gas chemistry)	Observed values (Bates *et al*., 1992)
5	3.67%	2.24%	2.9%
15	5.36%	3.41%	4.5%
25	8.43%	5.43%	11.9%
35	14.56%	10.08%	22.25%
45	21.16%	17.38%	33.2%
55	24.77%	23.46%	40.25%

References

Adewuyi, Y. G., 1989: Oxidation of biogenic sulfur compounds in aqueous media: Kinetics and environmental implications, in E. S. Saltzman and W. J. Cooper (eds), *Biogenic Sulfur in the Environment*, ACS Symposium Series 393, pp. 529–559.

Andreae, M. O., 1990: Ocean-atmosphere interaction in the global biogeochemical sulphur cycle, *Marine Chem.* **30**, 1–29.

Ayers, G. P., Cainey, J. M., Granek, H., and Leck, C., 1996: Dimethylsulfide oxidation and the ratio of methanesulfonate to non-sea-salt sulfate in the marine aerosol, *J. Atmos. Chem.* **25**, 307–325.

Barnes, I., Bastian, V., and Becker, K. H., 1988: Kinetic and mechanisms of the reaction of OH radicals with dimethyl sulfide, *Int. J. Chem. Kinet.* **20**, 415–431.

Barone, S. B., Turnipseed, A. A., and Ravishankara, A. R., 1995: Role of adducts in the atmospheric oxidation of dimethylsulphide, *Faraday Discussion* **100**, 39–54.

Bates, T. S. and Quinn, P. K., 1997: Dimethylsulphide (DMS) in the equatorial Pacific Ocean (1982 to 1996): Evidence of a climate feedback?, *Geophys. Res. Lett.* **24** (8), 861–864.

Bates, T. S., Calhoun, J. A., and Quinn, P. K., 1992: Variations in the methanesulfonate to sulfate molar ratio in submicrometer marine areosol particles over the South Pacific Ocean, *J. Geophys. Res.* **97**, 9859–9865.

Bates, T. S., Charlson, R. J., and Gammon, R. H., 1987: Evidence for the climatic role of marine biogenic sulphur, *Nature* **329**, 319–321.

Baulch, D. L., Cox, R. A., Crutzen, P. J., Hampson, R. F. Jr., Kerr, J. A., Troe, J., and Watson, R. T., 1982: Evaluation kinetic and photochemical data for atmospheric chemistry: Supplement I, *Phys. Chem. Ref. Data* **11**, 327–496.

Benkovitz, C. M., Berkowitz, C. M., Easter, R. C., Nemesure, S., Wagener, R., and Schwartz, S. E., 1994: Sulphate over the North Atlantic and adjacent continental regions: Evaluation for October and November 1986 using a three-dimensional model driven by observation-derived meteorology, *J. Geophys. Res.* **99**, 20725–20756.

Benson, S. W., 1978: Thermochemistry and kinetics of sulfur-containing molecules and radicals, *Chem. Rev.* **78**, 23–35.

Betterton, E. A., 1992: Oxidation of alkyl sulfides by aqueous peroxymonosulfate, *Env. Sci. Tech.* **26**, 527–532.

Byrd, R. B., Stewart, W. E., and Lightfoot, E. N., 1970: *Transport Phenomena*, Wiley and Sons.

Capaldo K. P. and Pandis, S. N., 1997: Dimethylsulphide chemistry in the remote marine atmosphere: Evaluation and sensitivity analysis of available mechanisms, *J. Geophys. Res.* **102**, 23251–23267.

Chameides, W. L. and Stelson, A. W., 1992: Aqueous-phase chemical processes in deliquescent sea-salt aerosols: A mechanism that couples the atmospheric cycles of *S* and sea salt, *J. Geophys. Res.* **97**, 20,565–20,580.

Charlson, R. J., Lovelock, J. E., Andreae, M. O., and Warren, S. G., 1987: Sulfur phytoplankton, atmospheric sulfur, cloud albedo and climate, *Nature* **326**, 655–661.

Charlson, R. J., Schwartz, S. E., Hales, J. M., Cess, R. D., Coakley, J. A., Jr., Hansen, J. E., and Hofmann, D. J., 1992: Climate forcing by anthropogenic aerosols, *Science* **255**, 423–430.

Clegg, S. L. and Brimblecombe, P., 1985: The solubility of methanesulphonic acid and its implications for atmospheric chemistry, *Environ. Tech. Lett.* **6**, 269–278.

Conover, W. J., 1980: *Practical Nonparametric Statistics*, 2nd ed., Wiley and Sons, New York.

Dacey, J. W. H., Wakeham, S. G., and Howes, B. L., 1984: Henry's law constant for dimethylsulfide in freshwater and seawater, *Geophys. Res. Lett.* **11**, 991–994.

Davis, D., Chen, G., Kasibhatla, P., Jefferson, A., Tanner, D., Eisele, F., Lenschow, D., Neff, W., and Berresheim, H., 1998: DMS oxidation in the Antarctic marine boundary layer: Comparison of model simulations and field observation of DMS, DMSO, $DMSO_2$, H_2SO_4(g), MSA(g), and MSA(p), *J. Geophys. Res.* **103**, 1657–1678.

De Bruyn, W. J., Shorter, J. A., Davidovits, P., Worsnop, D. R., Zahnisher, M. S., Kolb, C. E., 1994: Uptake of gas phase sulfur species methanesulfonic acid, dimethylsulfoxide, and dimethyl sulfone by aqueous surfaces, *J. Geophys. Res.* **99**, 16927–16932.

DeMore, W. B., Sander, S. P., Golden, D. M., Hampson, R. F., Kurylo, M. J., Howard, C. J., Ravishankara, A. R., Kolb, C. E., and Molina, M. J., 1994: Chemical kinetics and photochemical data for use in stratospheric modeling, Evaluation number 11, JPL publication, 94-26.

Dentener, F. J., 1993: Heterogeneous chemistry in the troposphere, PhD Tthesis, University of Utrecht, The Netherlands.

Dentener, F. J., 1994: Private communication.

Domine', F., Murrells, T. P., and Howard, C. J., 1990: Kinetics and mechanisms of the reactions of CH_3S, CH_3SO and CH_3SS with O_3 at 300 K and low pressure, *J. Phys. Chem.* **94**, 5839–5847.

Domine', F., Ravishankara, A. R., and Howard, C. J., 1992: 'Kinetics and mechanisms of the reactions of CH_3S, CH_3SO and CH_3SS with O_3 at 300 K and low pressure, *J. Phys. Chem.* **96**, 2171–2178.

Draper, N. R. and Smith, H., 1981: *Applied Regression Analysis*, Wiley and Sons, New York.

Falbe-Hansen, H., Sørensen, S., Jensen, N. R., Hjorth, J., 1998: Unpublished results.

Helton, J. C., 1993: Uncertainty and sensitivity analysis techniques for use in performance assessment for radioactive waste disposal, *Rel. Eng. System Safety* **42**, 327–367.

Helton, J. C., Garner, J. W., McCurley, R. D., and Rudeen, D. K., 1991: Sensitivity analysis techniques and results for the performance assessment at the waste isolation pilot plant, Sandia National Laboratories report SAND90-7103.

Hertel, O., Christensen, J., and Hov, Ø., 1994: Modelling of the end products of the chemical decomposition of DMS in the marine boundary layer, *J. Atmos. Env.* **28**, 2431–2449.

Homma, T. and Saltelli, A., 1991: PREP (Statistical Pre-Processor); Program description and user guide, CEC/JRC Scientifical and Technical Report, EUR 13922 EN, Luxemburg.

Hynes, A. J. and Wine, P. H., 1996: The atmospheric chemistry of dimethylsulfoxide (DMSO) kinetics and mechanism of the OH + DMSO reaction, *J. Atmos. Chem.* **24**, 23–27.

Hynes, A. J., Wine, P. H., and Semmes, D. H., 1986: Kinetics and mechanism of OH reactions with organic sulfides, *J. Phys. Chem.* **90**, 4148–4156.

Iman, R. L. and Helton, J. C., 1988: A comparison of uncertainty and sensitivity analysis techniques for computer models, *Risk Anal.* **8** (1), 71–90.

Iman, R. L., Helton, J. C., and Campbell, J. E., 1981: An approach to sensitivity analysis of computer models, Part I and II, *J. Qual. Tech.* **13** (3,4), 174–183 and 232–240.

Jefferson, A., Tanner, D. J., Eisele, F. L., Davis, D. D., Chen, G., Crawford, J., Huey, J. W., Torres, A. L., and Berresheim, H., 1998: OH photochemistry and methane sulphonic acid formation in the coastal Antarctic boundary layer, *J. Geophys. Res.* **103**, 1647–1656.

Jensen, N. R., Hjorth, J., Lohse, C., Skov, H., and Restelli, G., 1992: Products and mechanism of the gas phase reactions of NO_3 with CH_3SCH_3, CD_3SCD_3, CH_3SH and CH_3SSCH_3, *J. Atmos. Chem.* **14**, 95–108.

Koga, S. and Tanaka, H., 1993: Numerical study of the oxidation process of Dimethylsulphide in the marine atmosphere, *J. Atmos. Chem.* **17**, 201–228.

Koga, S. and Tanaka, H., 1996: Simulation of seasonal variations of sulfur compounds in the remote marine atmosphere, *J. Atmos. Chem.* **23**, 163–192.

Langner, J. and Rodhe, H., 1991: A global three-dimensional model of the tropospheric sulphur cycle, *J. Atmos. Chem.* **13**, 225–265.

Lee, Y. N. and Zhou, X., 1994: Aqueous reaction kinetics of ozone and dimethylsulfide and its atmosphere implications, *J. Geophys. Res.* **99**, 3597–3605.

Legrand, M. and Pasteur, E. C., 1998: Methane sulfonic acid to non-sea-salt sulfate ratio in coastal Antarctic aerosol and surface snow, *J. Geophys. Res.* **103**, 10,991–11,006.

Luria, M. and Sievering, H., 1991: Heterogeneous and homogeneous oxidation of SO_2 in the remote marine atmosphere, *J. Atmos. Environ.* **25A**, 1489–1496.

McArdle, J. V. and Hoffman, M. R., 1983: Kinetics and mechanism of the oxidation of aquated sulfur dioxide by hydrogen peroxide at low pH, *J. Phys. Chem.* **87**, 5425–5429.

Mellouki, A., Jourdan, J. L., and LeBras, G., 1988: Dioscharge flow study of the $CH_3S + NO_2$ reaction mechanism using $Cl + CH_3SH$ as the CH_3S source, *Chem. Phys. Lett.* **148**, 231–236.

Milne, P. J., Zika, R. G., and Saltzman, E. S., 1989: Oxidation of biogenic sulfur compounds in aqueous media: Kinetics and environmental implications, in E. S. Saltzman and W. J. Cooper (eds), *Biogenic Sulfur in the Environment*, ACS Symposium Series 393, pp. 518–528.

Moore, W. J., 1978: *Physical Chemistry*, Longman, London, p. 289.

Olson, T. M. and Fessenden, R. W., 1992: Pulse radiolysis study of the reaction of OH radicals with methanesulfonate and hydroxymethanesulfonate, *J. Phys. Chem.* **96**, 3317–3320.

Oort, A. H., 1983: Global atmospheric circulation statistics 1958–1973, NOAA Professional Paper No. 14, U.S. Government Printing Office, Washington, D.C.

Oreskes N., Shrader-Freschette, K., and Belitz, K., 1994: Verification, validation and confirmation of numerical models in the earth sciences, *Science* **263**, 641–646.

Pandis, S. N. and Seinfeld, J., 1989: Sensitivity analysis of a chemical mechanism for aqueous-phase atmospheric chemistry, *J. Geophys. Res.* **94**, 1105–1126.

Penner, J. E., Dickinson, R., and O'Neill, C., 1992: Effects of aerosol from biomass burning on the global radiation budget, *Science* **256**, 1432–1434.

Penner, J. E., Ghan, S. J., and Walton, J. J., 1991: The role of biomass burning in the budget and cycle of carbonaceous soot aerosols and their climate impact, in. J. Levine (ed.), *Global Biomass Burning*, MIT Press, Cambridge, MA, pp. 387–393.

Pham, M., Muller, J.-F., Brasseur, G. P., Granier, C., and Megie, G., 1995: A three-dimensional study of the tropospheric sulphur cycle, *J. Geophys. Res.* **100**, 26061–26092.

Pruppacher, H. R., and Klett, J. D., 1980: *Microphysics of Clouds and Precipitation*, D. Reidel Publishing Company, Dordrecht, Holland.

Raes, F., 1995: Entrainment of free tropospheric aerosols as a regulating mechanism for cloud condensation nuclei in the remote marine boundary layer, *J. Geophys. Res.* **100**, 2893–2903.

Ray, A., Vassalli, I., Laverdet, G., and LeBras, G., 1996: Kinetics of the thermal decomposition of the CH_3SO_2 radical and its reaction with NO_2 at 1 Torr and 298 K, *J. Phys. Chem.* **100**, 8895–8900.

Remedio, J. M., Saltelli, A., Hjorth, J., and Wilson, J., 1994: KIM. A chemical kinetic model of the OH-initiated oxidation of DMS in air: A Monte Carlo analysis of the latitude effect, EUR Report 1994 EN.

Saltelli, A. and Hjorth, J., 1995: Uncertainty and ensitivity analyses of OH-initiated dimethylsulphide (DMS) oxidation kinetics, *J. Atmos. Chem.* **21**, 187–221.

Saltelli, A. and Homma, T., 1991: SPOP; Program description and user guide, CEC/JRC Scientifical and Technical Report, EUR 13924 EN, Luxemburg.

Saltelli, A. and Homma, T., 1992: Sensitivity analysis for model output; Performance of black box techniques on three international benchmark exercises, *Comp. Stat. Data Anal.* **13** (1), 73–94.

Saltelli, A. and Marivoet, J., 1990: Nonparametric statistics in sensitivity analysis for model output; A comparison of selected techniques, *Rel. Eng. System Safety* **28**, 229–253.

Saltelli, A., Andres, T. H., and Homma, T., 1993: Sensitivity analysis of model output; An investigation of new techniques, *Comp. Stat. Data Anal.* **15**, 211–238.

Saltzman, E. S., Savoie, D. L., Prospero, J. M., and Zika, R. G., 1986: Methane sulfonic acid and non-sea-salt sulfate in Pacific air: Regional and seasonal variations, *J. Atmos. Chem.* **4**, 227–240.

Savoie, D. L. and Prospero, J. M., 1989: Comparison of oceanic and continental sources of non-sea-salt sulphate over the Pacific Ocean, *Nature* **339**, 685–689.

Schwartz, S. E., 1988: Are global cloud albedo and climate controlled by marine phytoplankton?, *Nature* **336**, 441–445.

Seinfeld, J., 1986: *Air Pollution*, Wiley and Sons, New York.

Shaw, G. E., 1983: Bio-controlled thermostasis involving the sulphur cycle, *Clim. Change* **5**, 297–303.

Sørensen, S., Falbe-Hansen, H., Mangoni, M., Hjorth, J., and Jensen, N. R., 1996: Observation of DMSO and $CH_3S(O)OH$ from the gas phase reaction between DMS and OH, *J. Atmos. Chem.* **24**, 299–315.

Spiro, P. A., Jacob, D. J., and Logan, J. A., 1992: Global inventory of sulfur emissions with $1^\circ \times 1^\circ$ resolution, *J. Geophys. Res.* **97**, 6023–6036.

Turanyi, T., 1990: Reduction of large reaction mechanisms, *New J. Chem.* **14**, 795–803.

Turnipseed, A. A. and Ravishankara, A. R., 1993: The atmospheric oxidation of dimethyl sulfide: Elementary step in a complex mechanism, in G. Restelli and G. Angeletti (eds), *Proceeding of the International Symposium 'Dimethylsulfide, Ocean, Atmosphere and Climate'*, Kluwer, Dordrecht, pp. 185–196.

Turnipseed, A. A., Barone, S. B., and Ravishankara, A. R., 1992: Observation of CH_3S addition to O_2 in the gas phase, *J. Phys. Chem.* **96**, 7502–7505.

Turnipseed, A. A., Barone, S. B., and Ravishankara, A. R., 1993: Reactions of CH_3S and CH_3SOO with O_3, NO_2, and NO, *J. Phys. Chem.* **97**, 5926–5934.

Tyndall, G. S., and Ravishankara, A. R., 1989: Kinetic and mechanism of the reactions of CH_3S with O_2 and NO_2 at 298 K, *J. Phys. Chem.* **93**, 2426–2435.

Tyndall, G. S. and Ravishankara, A. R., 1991: Atmospheric oxidation of reduced sulfur species, *Int. J. Chem. Kinet.* **23**, 483–527.

Van Dingenen, R., Jensen, N. R., Hjorth, J., and Raes, F., 1994: Peroxynitrate formation during the night-time oxidation of dimethylsulphide: its role as a reservoir species for aerosol formation, *J. Atmos. Chem.* **18**, 211–237.

Watts, S. F. and Brimblecombe, P., 1987: The Henry's law constant of dimethylsulfoxide, *Env. Sci. Tech.* **8**, 483–486.

Yin, F., Grosjean, D., and Seinfeld, J. H., 1990a: Photooxidation of dimethyl sulfide and dimethyl disulfide I: Mechanism development, *J. Atmos. Chem.* **11** (4), 309–364.

Yin, F., Grosjean, D., Flagan, R. C., and Seinfeld, J. H., 1990b: Photooxidation of dimethyl sulfide and dimethyl disulfide. II: Mechanism evaluation, *J. Atmos. Chem.* **11** (4), 365–399.

Zimmerman, P. H., 1984: Ein dreidimensionales, numerishes Transportmodell für atmosphärische Spurenstoffen, PhD Thesis University of Mainz, FRG.

Zimmerman, P. H., Feichter, J., Wrath, H. K., Crutzen, P. J., and Weiss, W., 1989: A global three dimensional source-receptor modle investigation using ^{85}Kr, *Atmos. Environ.* **23**, 25–35.